 DOI: 10.1111/risa.12475

Binary Mixtures of Polycyclic Aromatic Hydrocarbons Display Nonadditive Mixture Interactions in an *In Vitro* Liver Cell Model

Stacey J. Gaskill[1] and Erica D. Bruce[2,*]

Polycyclic aromatic hydrocarbons (PAHs) have been labeled contaminants of concern due to their carcinogenic potential, insufficient toxicological data, environmental ubiquity, and inconsistencies in the composition of environmental mixtures. The Environmental Protection Agency is reevaluating current methods for assessing the toxicity of PAHs, including the assumption of toxic additivity in mixtures. This study was aimed at testing mixture interactions through *in vitro* cell culture experimentation, and modeling the toxicity using quantitative structure-activity relationships (QSAR). Clone-9 rat liver cells were used to analyze cellular proliferation, viability, and genotoxicity of 15 PAHs in single doses and binary mixtures. Tests revealed that many mixtures have nonadditive toxicity, but display varying mixture effects depending on the mixture composition. Many mixtures displayed antagonism, similar to other published studies. QSARs were then developed using the genetic function approximation algorithm to predict toxic activity both in single PAH congeners and in binary mixtures. Effective concentrations inhibiting 50% of the cell populations were modeled, with $R^2 = 0.90$, 0.99, and 0.84, respectively. The QSAR mixture algorithms were then adjusted to account for the observed mixture interactions as well as the mixture composition (ratios) to assess the feasibility of QSARs for mixtures. Based on these results, toxic addition is improbable and therefore environmental PAH mixtures are likely to see nonadditive responses when complex interactions occur between components. Furthermore, QSAR may be a useful tool to help bridge these data gaps surrounding the assessment of human health risks that are associated with PAH exposures.

KEY WORDS: Binary mixtures; *in vitro* cell culture; mixture interactions; polycyclic aromatic hydrocarbons (PAHs); risk assessment

1. INTRODUCTION

Polycyclic aromatic hydrocarbons (PAHs) are common environmental pollutants that are produced by natural and anthropogenic sources. Due to the nature of their production, PAHs occur as complex mixtures in environmental matrices. PAHs are formed by incomplete combustion of organic materials and naturally occur in petrogenic mixtures.[1–3] The class of PAHs is composed of hundreds of parent and substituted congeners. Alkylated and methylated congeners, for example, are common substituted PAHs that are formed in the same way

[1]Department of Environmental Science, Baylor University, One Bear Place #97266, Waco, TX, USA.
[2]Department of Environmental Science, Institute of Biomedical Studies, The Institute of Ecological, Earth, and Environmental Science, Baylor University, One Bear Place #97266, Waco, TX, USA.
*Address correspondence to Erica D. Bruce, Department of Environmental Science, Institute of Biomedical Studies, The Institute of Ecological, Earth, and Environmental Science, Baylor University, One Bear Place #97266, Waco, TX 76798–7266, USA; tel: (254) 710-4877; fax: (254) 710–3409; erica_bruce@baylor.edu.

 0272-4332/15/0100-0001$22.00/1

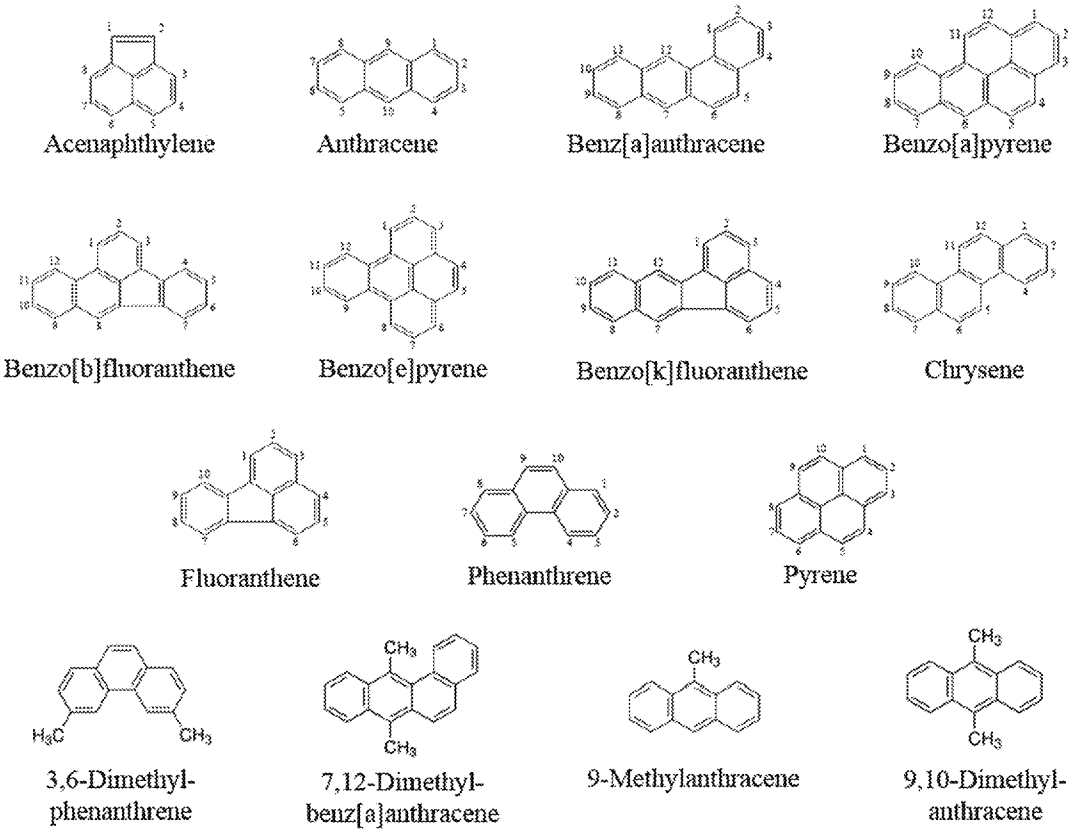

Fig. 1. Common parent and methylated PAH congeners.[6]

that parent congeners are formed.[4] See Fig. 1 for examples of common parent and methylated PAHs. Alkylated PAHs constitute a significant portion of some environmental mixtures, with some petrogenic mixtures containing more than 50% of the PAH fraction.[5]

Because PAHs are ubiquitous in the environment, humans are exposed to PAHs on a daily basis in food, air, dust, soil, and water.[6] Less than 20 parent PAH congeners are regularly monitored and analyzed by state and federal agencies.[6] Seven of these regularly monitored PAHs are classified as probable human carcinogens (termed cPAHs). The International Agency for Research on Cancer (IARC) has a widely used classification system that categorizes the carcinogenic potential of chemicals, although many PAHs are not yet classified because of a lack of available data.[6,7] Group 1 chemicals are carcinogenic to humans; Group 2A chemicals are probably carcinogenic; Group 2B chemicals are possibly carcinogenic; Group 3 chemicals are not yet classified. And finally, Group 4 chemicals are probably not carcinogenic to humans.[6,7] cPAHs serve as markers for estimating risks associated with human exposures.[7] The Environmental Protection Agency (EPA) has categorized two different methodologies for characterizing risks: a mixture-based approach, and a component-based approach. Mixture-based approaches utilize toxicologically characterized mixtures (diesel emissions, tobacco smoke, coke oven emissions, etc.) to estimate the relative toxicity of an environmental mixture.[8] The component-based approach assigns relative potency factors (RPFs) to the seven cPAHs, using benzo[a]pyrene (BaP) as the index chemical with a factor of 1. RPFs are being developed for many other PAHs to include in risk assessments.[9] The RPF approach makes two key assumptions: (1) PAHs in mixtures act via the same mode of action and (2) that mixture interactions do not occur and therefore toxicity is additive.[8] The RPF approach has two important weaknesses; the lack of incorporation of unanalyzed components in a PAH mixture, such as alkylated PAHs, and the assumption that mixture interactions are not occurring.[9]

Table I. Various Physical and Chemical Properties of Selected PAHs[10]

Chemical	Abbreviations	Rings	Molar Mass (g/mol)	IARC Cancer Group	$LogK_{ow}$
Acenaphthylene	Acy	3	152.2		4.07
Anthracene	Ac	3	178.2	3	4.50
Benz[a]anthracene	BaA	4	228.3	2B	5.91
Benzo[a]pyrene	BaP	5	252.3	1	6.06
Benzo[b]fluoranthene	BbF	5	252.3	2B	5.78
Benzo[e]pyrene	BeP	5	252.3	3	6.44
Benzo[k]fluoranthene	BkF	5	252.3	2B	6.11
Chrysene	Ch	4	228.3	2B	5.86
Fluoranthene	Fla	4	202.2	3	4.90
Phenanthrene	Phe	3	178.2	3	4.52
Pyrene	Pyr	4	202.2	3	4.88
3,6-Dimethyl-phenanthrene	3,6-Phe	3	206.3		5.44
7,12-Dimethyl-benz[a]anthracene	7,12-BaA	4	256.3		5.80
9-Methylanthracene	9-Ac	3	192.3		5.07
9,10-Dimethylanthracene	9,10-Ac	3	206.3		5.13

The majority of PAHs lack toxicological data, making risk assessment difficult and potentially less accurate.[10] Other studies have been conducted to assess potential mixture interactions in simple and complex PAH mixtures, with the majority assessing genotoxicity.[11–13] The only trend that has yet to be established is that PAH interactions appear erratic, with clear impacts on toxicity and genotoxicity of test organisms that do not equal the sum of the congeners.[11] Evidence suggests that the chosen test system is an influential factor in the toxicological response, and it is difficult to compare and draw relationships across various studies utilizing different test systems.[14–16]

Kang *et al.* tested environmental PAH mixtures extracted from indoor dust collected from schools, shopping malls, offices, factories, and manufacturing plants.[17] The study found that cytotoxicity was influenced by dose, mixture composition, and source.[17] Jarvis *et al.* performed an *in vitro* cell culture study comparing the DNA damage of a PAH mixture extracted from soil samples to a solitary BaP solution.[18] BaP-exposed cells were able to recover from and repair DNA damage; however, the cells exposed to the PAH mixtures showed significantly more DNA damage and decreased ability to recover and repair themselves.[18] A different study observed antagonism: BaP and dibenzo[a,l]pyrene displayed significantly higher levels of adduct formation in breast cancer MCF-7 cells than in trials where they were cotreated with a standard reference coal tar mixture, indicating antagonistic interactions within the complex mixture.[19]

These studies have highlighted several data gaps in PAH research, including the toxic potential of single PAHs, mixture interactions, and the variability of environmental mixtures. Relatively little research has been conducted on complex mixtures, simple PAH mixtures, or even many single PAHs. Because such research is costly and slow, alternative toxicology tools can be useful for chemicals such as PAHs. Quantitative structure-activity relationships (QSAR) modeling can help predict the toxicological or physical action of chemicals that lack data. QSARs can utilize molecular properties (called descriptors) of PAHs to predict various biological activity like toxic action.[15,20] QSAR modeling is an important step for understanding new chemicals, and is often used during the chemical screening process.[21]

The premise of this study is to test interactions that may occur between PAHs in simple mixtures. This study investigates these relationships by performing *in vitro* toxicological analyses with 15 selected parent and methylated PAHs (see Table I) in single concentrations and in various combinations of binary mixtures. Mixture analyses will be performed to ascertain the type of mixture interactions (additive, antagonistic, synergistic) that are present. Finally, various QSAR models will be developed to evaluate the potential ability of QSARs to predict the toxicological action of PAHs, both in single concentrations and in mixtures. These techniques will help risk assessors to better characterize the interactions in mixtures of PAHs and thus make more accurate predictions of human health risk from exposures.

2. METHODS

2.1. Materials

Normal rat liver Clone-9 cells were obtained from the American Type Culture Collection (ATCC) (Manassas, VA, USA) CRL 1439 passage 17, for *in vitro* cell culture. Nutrient HAMs F-12 mixture, serum-free Dulbecco's Modified Eagle Medium F-12, Dulbecco's phosphate buffer saline (PBS), HEPES, penicillin–streptomycin hybri-max, sodium bicarbonate, and dimethyl sulfoxide (DMSO) were obtained from Sigma-Aldrich (St. Louis, MO, USA). Trypsin–EDTA solution was obtained from Atlanta Biologicals (Lawrenceville, GA, USA). Fetal bovine serum (FBS) was obtained from Equitech-Bio (Kerrville, TX, USA).

Acenaphthylene, anthracene, benz[a]anthracene, benzo[a]pyrene, benzo[b]fluoranthene, benzo[e]pyrene, benzo[k]fluoranthene, chrysene, fluor anthene, phenanthrene, pyrene, 9-methylanthracene, 3,6-dimethylphenanthrene, 7,12-dimethylbenz [a]anthracene (DMBA), and 9,10-dimethylanthracene analytical standards (purity > 97%) were purchased from AccuStandard (New Haven, CT, USA). Janus Green B (JG) dye, 5-carboxyfluorescein diacetate acetoxymethyl ester (CFDA), acridine orange (AO) base, and 4',6-diamidino-2-phenylindole dihydrochloride (DAPI) were obtained from Sigma-Aldrich.

2.2. Methods

2.2.1. Cell Culture

Cells were maintained in Nutrient HAMs F-12 mixture, with 10% FBS, 1% penicillin-streptomycin solution, and 1420 M HEPES buffering agent. Cells were cultured in an incubator at 37 °C in 5% CO_2 and 90% humidity. The cells were grown to confluence in culture-treated sterile 75 cm^2 flasks. Once confluent, the cells were rinsed with PBS, detached with 0.25% trypsin and 0.53 mM EDTA solution, centrifuged, and counted using a Beckman Coulter particle counter. The cells were resuspended in media and then reseeded in transparent 96 multiwell plates or black 96 multiwell plates at approximately 5,000 cells/well. For the micronucleus (MN) assay, cells were reseeded in 6 or 12 multiwell plates at approximately 100,000 cells/well and 50,000 cells/well. The cells were allotted 24 hours to adhere to the plates and reach 50% confluence before dosing.

2.2.2. Chemical Dosing

All 15 PAHs were dissolved in DMSO in sterilized amber vials. Trials were completed within 10 cell passages of being received from ATCC. Single PAH dosing trials were randomized across the plates, with a control, vehicle control, and PAH doses ranging from 0.25 parts per million (ppm) to 10 ppm dissolved in 0.5% DMSO. For the binary mixtures, BaP, together with one of the other 14 PAHs, were dissolved in 0.5% DMSO in the media. Binary mixtures were divided into two separate trials: binary and reverse binary mixtures. In binary mixtures, BaP was held constant at 1 ppm and the concentration of the other PAH varied (0.25–10 ppm). In reversed binary mixtures, BaP concentrations varied (1–10 ppm) and the other PAH remained constant at 1 ppm.

2.2.3. Cytotoxicity

Following chemical exposures, cytotoxicity was assessed by examining cellular proliferation and viability. JG dye was used to assess cellular proliferation.[22] CFDA was used to assess viability. After 24-hour chemical exposures, assays were performed. The cell media was aspirated from all wells, followed by two gentle rinses of PBS. JG proliferation and viability assays were performed simultaneously in clear 96 well plates. For proliferation, the wells were fixed in ethanol for 90 seconds. JG dye was made up in 1 mg/mL PBS solution and then all wells were dyed for 60 seconds. The wells were rinsed twice more in PBS and then aspirated to completely remove all liquid. Wells were resuspended in 100 μL of ethanol and 100 μL of nanopurified water and then the plates were quantified using a BioTek microplate spectrophotometer at 590 nm.

To perform CFDA assay, first all cell media was aspirated and every well was rinsed twice with warm PBS++. CFDA was dissolved in DMSO, and then added to warm, serum-free media, making up a final concentration of 4 μM on the cells. The plate was then incubated for 30 minutes to allow the CFDA to permeate the cells. The cells were then rinsed twice and resuspended with warm serum-free Dulbecco's Modified Eagle Medium media. The plates were immediately quantified using a Fluoroskan Ascent microplate fluorometer, with emission/excitation at 485/538 nm.

2.2.4. Genotoxicity

The MN test was chosen for the evaluation of carcinogenic potency. The MN test measures

Fig. 2. Cells were imaged at 20× magnification using DAPI fluorescence.

genotoxicity by detecting micronuclei in cells during or after mitotic division. Micronuclei are inappropriate pieces of DNA that have failed to migrate properly during cell division and signify genetic damage. Two probes were used: the DAPI DNA probe, and AO RNA/DNA probe to illuminate nuclei, micronuclei, cytoplasmic material, and apoptotic bodies for scoring.

Protocol and scoring for the MN test were adapted from Fenech *et al.*[23,24] All trials were performed at cell passage 24. Before chemical dosing, the cells were submerged in serum-free warm media for two hours. Serum starvation synchronizes the cell cycles of the population to maximize scoring. The cells were then dosed in regular HAMs F12 media with chemical and given 24 hours to complete at least one cell division. Trials include control groups, solvent control groups, two single chemical groups (1 ppm and 10 ppm), and various combinations of binary mixtures. Chrysene was tested at 0.25 ppm and 1 ppm to achieve solution.

The DAPI probe was prepared at 300 nM in warm PBS stock solution. AO was dissolved in 0.1 M citric acid and then 0.2 M Na_2HPO_4 was added to make up the AO stain solution. The wells were rinsed and incubated with AO stain solution for 30 minutes. The wells were rinsed and fixed with ethanol. The plates were then incubated with the DAPI dye solution for five minutes. Plates were scored using fluorescence microscopy at 20× magnification (Fig. 2).

Nuclear fragments were scored as micronuclei if they were less than one-third the diameter of the main nuclei (Fig. 3). Abnormal, apoptotic, and necrotic cells were excluded from the MN statistical analyses, but were observed only to quantify cell death within the chemical doses (Fig. 4).

2.2.5. Statistical Analyses

All statistical analyses were performed using Microsoft Excel and Sigmaplot 11.0 software from Systat. A Student's *t*-test was used for cytotoxicity data. The assigned alpha value was 0.05 to determine statistical significance of p values.

MN count data were converted into proportions of micronucleated cells per 1,000 cells in each sample, as described by Matsushima *et al.* and Fenech *et al.*[23,24] The Mann-Whitney rank test was chosen because the data are not normally distributed and it has been used effectively in other published work with micronuclei tests.[24,25] Dosing groups were compared to their own control group per plate, and MN frequencies varied from plate to plate. If there was a p value <0.05, the dosing group was assigned a positive result for causing significant genotoxicity. It should be noted that if a p value was less than 0.05 but skewed left, it was automatically assigned a negative result because genotoxicity is not present.

2.2.6. Mixture Analyses

The EPA's 1986 guidelines for the assessment of chemical mixtures contain models for analyzing the interactions of chemicals within simple mixtures, originally developed by Finney in 1942, and used to analyze interactions in each chemical ratio.[26] The model determines if a mixture's dose-response relationship displays a synergistic, antagonistic, or additive chemical interaction when the mixture is compared to the dose-response information of the individual components.[27] The interactions were also analyzed using a common dose-additive comparison.

2.2.7. QSAR Modeling

Discovery Studio 4.0 (Accelrys) was used to develop QSAR models. The chosen biological end point was the effective chemical concentration that reduced the percentage of viable cells by 50% (EC_{50}), which was approximated using linear regression of the CFDA data. The genetic function approximation algorithm was used to determine the best predictive model for PAHs' EC_{50}. Three major parameters were used to analyze the model's accuracy: correlation coefficient (R^2), adjusted correlation coefficient (R^2(adj)), and lack of fit (LOF). R^2 is a percentage that describes how well the predicted values represent the experimental data. R^2 (adj) uses the same basic premise, except it is a smoothed number that may exclude data points that are highly

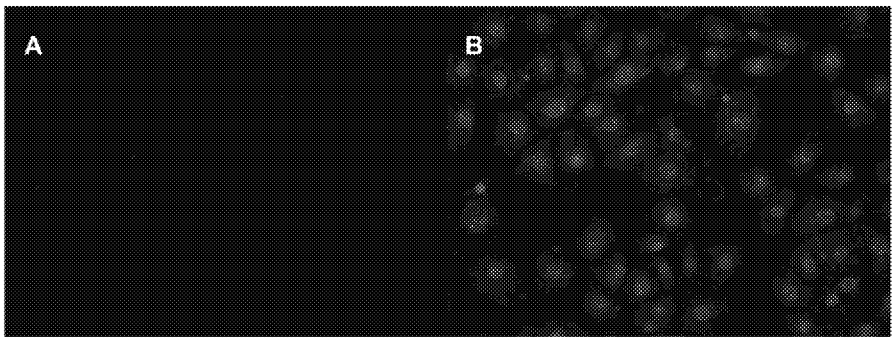

Fig. 3. A 20× magnified K-9 cell is shown with two different contrasts. (A) Only DAPI is shown where MN are identified. (B) AO is used to illuminate cell boundaries.

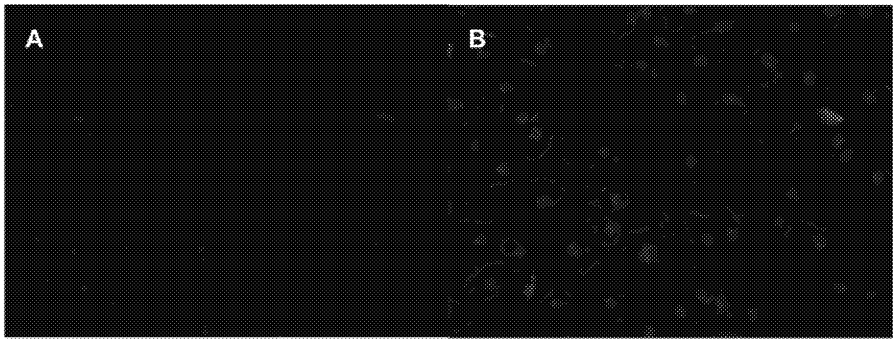

Fig. 4. Examples of cells that do not meet scoring criteria. Many of these cells are undergoing cell death because their DNA was seen outside their nuclei and lacked clear membrane boundaries.

skewed. LOF measures the probability of accurately predicting the EC_{50} of doses and thus the higher the probability, the more accurate the model. Three models were developed, each employing the EC_{50} of single PAHs, binary mixtures, and the reverse binary mixtures.[14] For each model, a training set of PAHs (using EC_{50} data points) is used and then the model is tested and validated using the remaining data points. In the single trials, three PAH EC_{50}s were selected for training the model, and the remaining 12 comprised the test set. In mixtures, there are only 11 remaining data points in the test set. After the most accurate models are selected, the algorithms for the mixtures are modified to incorporate the component ratios within the mixture, as adapted from Altenburger *et al.*[14]

3. RESULTS

3.1. Cytotoxicity

3.1.1. Proliferation

Fig. 5 displays the cytotoxicity results for all chemicals. Anthracene, benzo[e]pyrene, benzo[k] fluoranthene, and chrysene showed no statistical difference from control groups in single trials. However, binary trials of these chemicals showed different trends. The statistical differences observed in anthracene trials were increases seen in three doses of the reverse binary trial. The statistically significant response seen in benzo[e]pyrene mixtures occurred in the reverse binary trial's two highest doses. All benzo[k]fluoranthene mixture data had no trending effect on the proliferation of the cells. The chrysene binary trial showed a statistical decline in the highest dose while the reverse binary trial showed an increase in proliferation in the two highest doses.

Acenaphthylene, benz[a]anthracene, fluoranthene, and 9-methylanthracene all displayed a statistical decline in single trials in one or two doses (Fig. 5). Acenaphthylene mixtures did not see any statistical decline but several doses showed statistical increases. The mixture data of benz[a]anthracene showed no evidence of a decline in proliferative capability of cells. Statistical increases in proliferation were observed in two doses of the benz[a]anthracene mixture data. In fluoranthene mixtures, no decline in proliferative capability was observed. The binary trial showed an increase in the highest dose, and the reverse binary trial showed a statistical

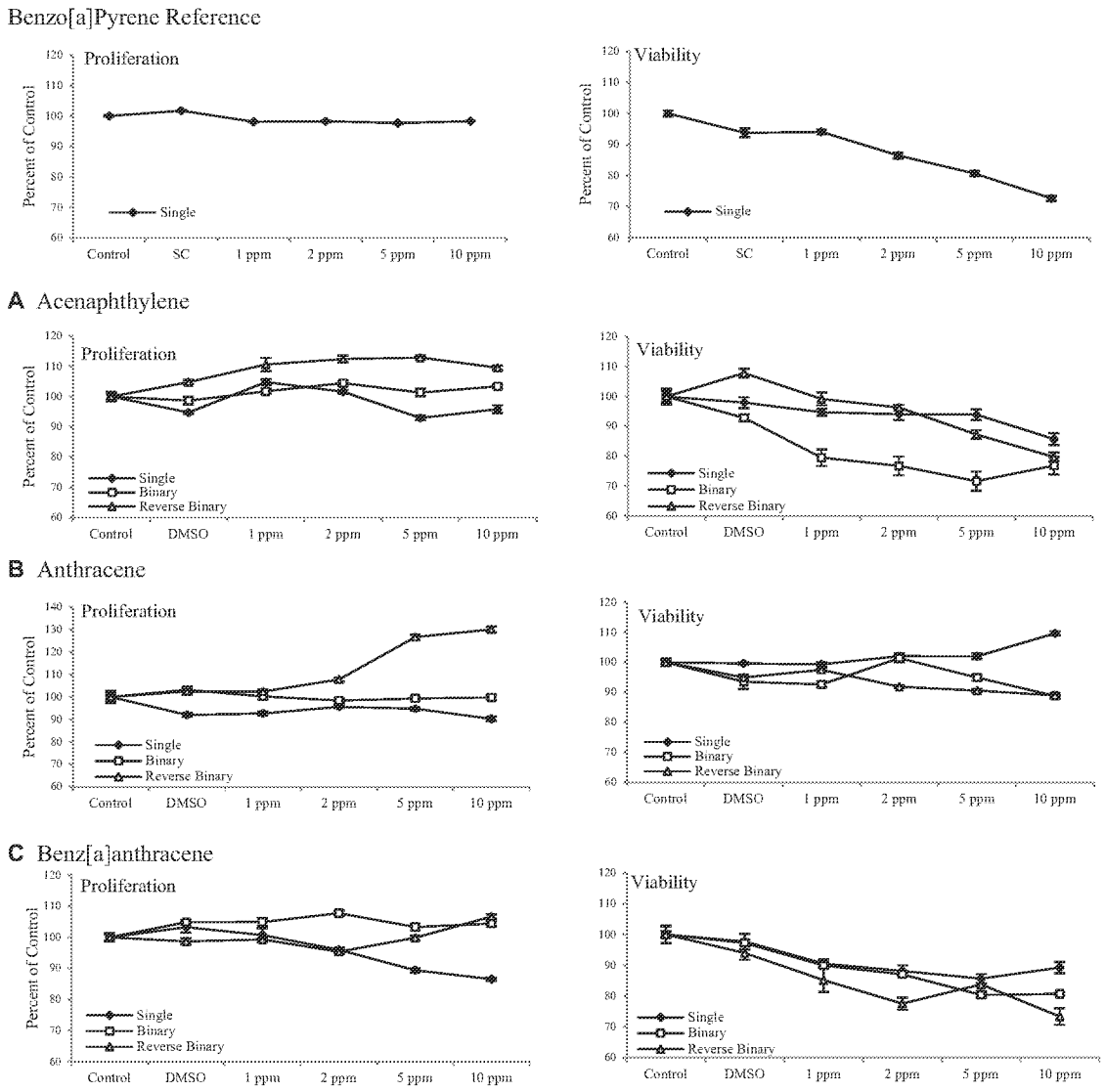

Fig. 5. The cytotoxicity results of 15 single PAHs in single concentrations and various binary mixture ratios. The results are displayed as percentages relative to control groups. Declining trends correspond with an observable decline both for proliferation and viability of cells.

increase in the two highest doses. In mixture trials of 9-methylanthracene, the only significant statistical difference was a decline in the highest doses.

Some single PAHs caused a statistical decline in proliferation in at least three doses, and include benzo[b]-fluoranthene, DMBA, 3,6-dimethyl-phenanthrene, and 9,10-dimethyl-anthracene. The benzo[b]fluoranthene binary trial showed a severe response, with all four doses significantly impairing the growth of cells. The BbF reverse binary trial did not cause a decline, but the cell populations in two subsequent doses were significantly higher than the control groups. DMBA binary trial did not have any dosing groups that were statistically different from the control. In the 7,12-BaA reverse binary trial, the three highest doses showed statistical decline. 3,6-Dimethylphenanthrene trials showed a less severe response, with declines in the two highest doses in binary. The reverse binary trial showed no decline in proliferation. Both binary trials of 9,10-dimethylanthracene displayed a diminished effect on proliferation, with significance only in the highest dose in the first trial. Phenanthrene and pyrene caused significant increases in proliferation of cells exposed to single concentrations. Similarly, all phenanthrene mixtures caused an increase in

D Benzo[b]fluoranthene

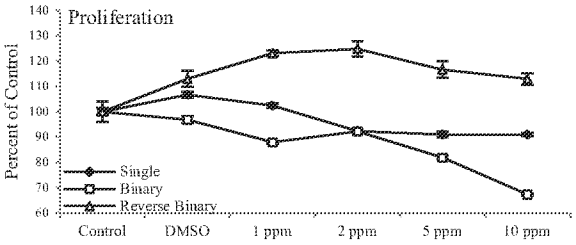

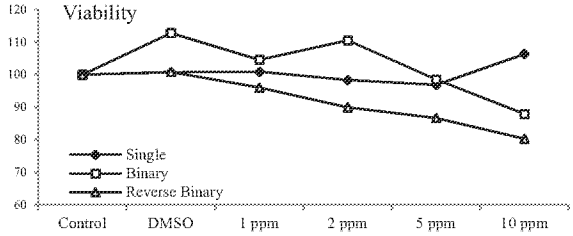

E Benzo[e]pyrene

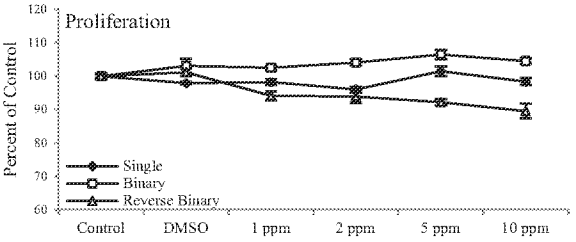

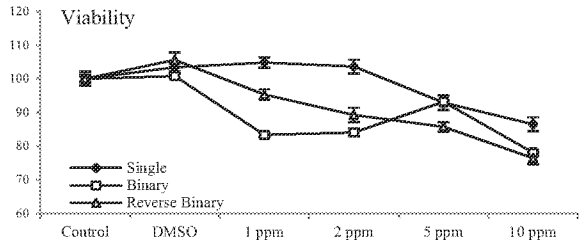

F Benzo[k]fluoranthene

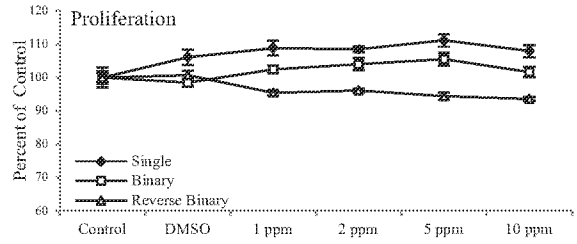

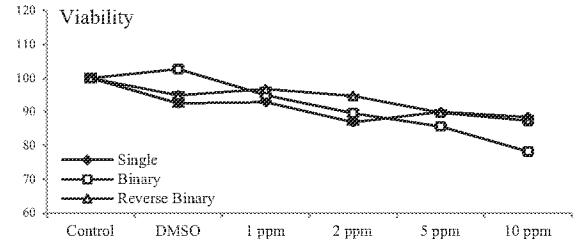

G Chrysene

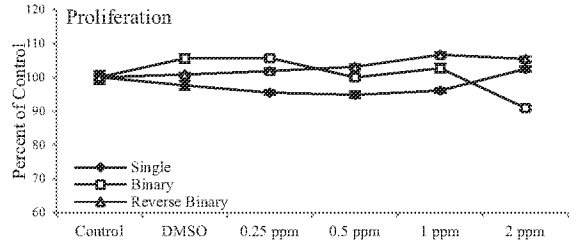

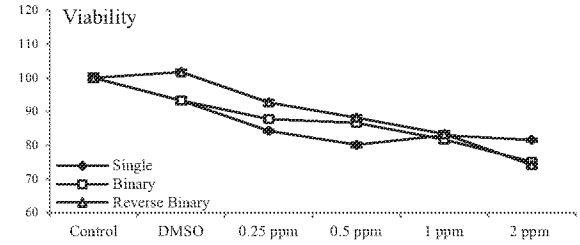

H Fluoranthene

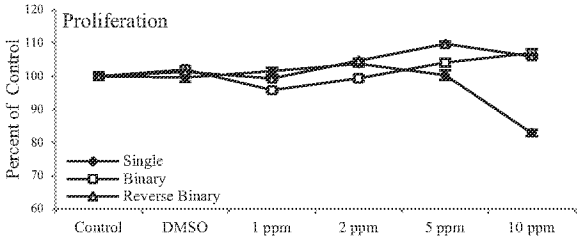

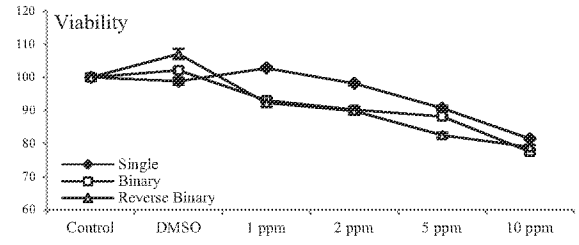

Fig. 5. Continued.

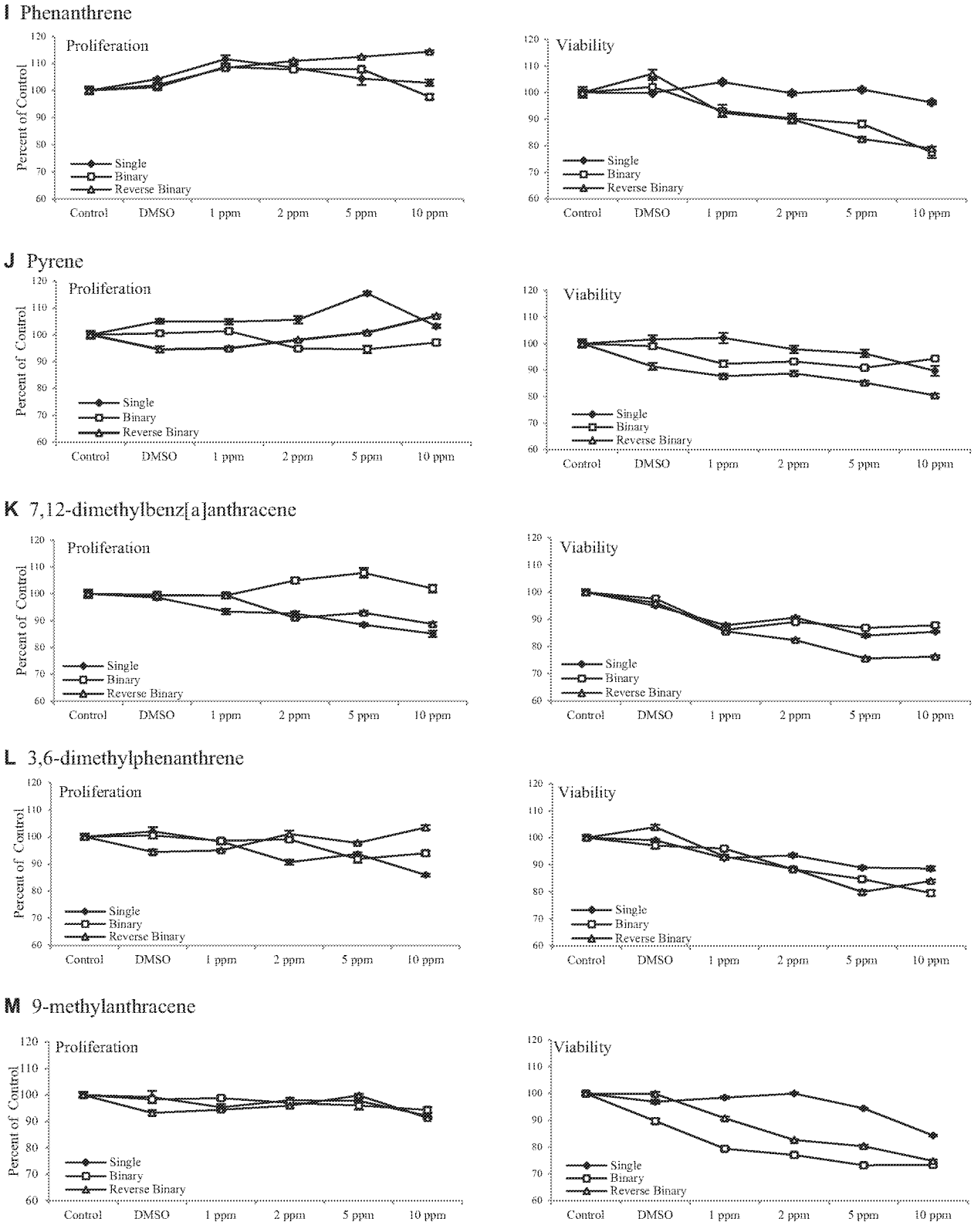

Fig. 5. Continued.

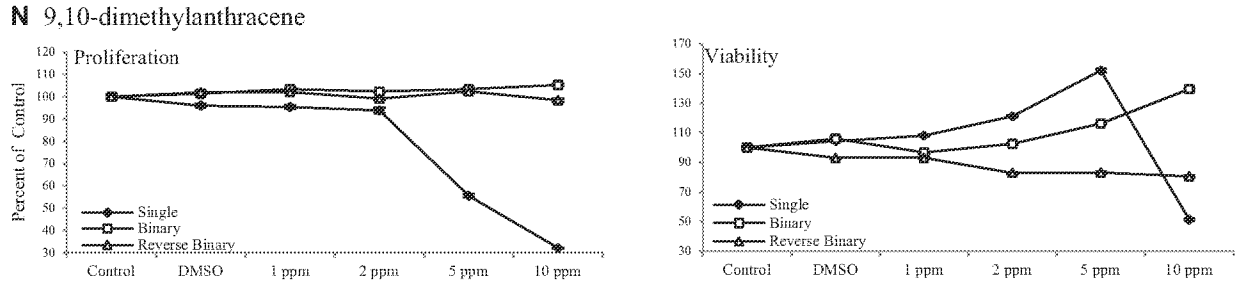

Fig. 5. Continued.

proliferation in the majority of doses. Pyrene mixtures trials showed no decline in proliferation but one dose showed significant increase. Table II is a summary chart of the findings and organizes the results using the statistical significance to see trending effects.

3.1.2. Viability

Single trials of acenaphthylene, anthracene, benzo[b]fluoranthene, benzo[e]pyrene, fluoranthene, pyrene, and 9-methylanthracene displayed statistical declines in one or two doses (Fig. 5). Acenaphthylene binary data showed a statistical decline in three dosing groups, and reverse binary in two dosing groups. The anthracene binary data reveal that the cells appeared as viable as the control cells in all doses except for the 10 ppm dose. Reverse binary data showed a dose-dependent statistical decline in viability in the three highest doses. Benzo[b]fluoranthene in the binary trial did not inhibit the viability of cells in any dosing groups. When the concentration of BaP varied, however, there was a statistically significant response, with viability inhibited in the three highest doses of BbF. In both binary mixtures of benzo[e]pyrene, the three highest doses were statistically less viable than the control groups. The fluoranthene binary trial caused a statistical decline in the three highest doses, and the reverse binary trial in the two highest doses. Pyrene binary trials showed statistical declines in the two highest doses of the reverse trial. In both binary trials of 9-methylanthracene, the three highest doses were statistically lower than the control groups.

Benz[a]anthracene, benzo[k]fluoranthene, chrysene, DMBA, and 3,6-dimethylphenanthrene showed statistical declines in three or four dosing groups. Both the binary and reverse binary of benz[a]anthracene trials showed decline in the three highest doses. Benzo[k]fluoranthene binary mixtures caused a statistical decline in viability in three doses, and the reverse binary trial showed the two highest doses significantly lower than control groups. Both chrysene trials showed a decline in the three highest doses. In DMBA mixtures, all doses had significantly fewer viable cells than their control groups. 3,6-Dimethylphenanthrene showed a similar trend, where the mixtures showed a significant statistical decline in the three highest doses.

The single trial of 9,10-dimethylanthracene did not display a dose-dependent relationship. Dosing groups showed a statistical increase in proliferation, followed by a sharp statistical decline and rapid death in the highest dose. The binary trial showed a statistical increase in the two highest doses. The reverse binary trials, however, displayed a dose-dependent relationship with a significant statistical decline in the three highest doses. Table III shows the trending results for the viability trials and is organized based on statistical significance.

3.2. Genotoxicity

The results for the MN assay are displayed in Table IV. The table shows the average micronuclei frequency per 1,000 cells in the sample population at all doses. The data are organized by the single concentrations tested, and the various binary mixtures of 14 PAHs with BaP. If a p value was <0.05, the dosing group was assigned a positive result and the chemical or mixture is interpreted as causing significant genotoxicity when compared to the control group. Negative results were assigned when the frequencies of the doses were insignificant to the control groups and if the MN frequency was skewed left. Overall, the genotoxicity trials were in agreement with other similar studies.[24,28] For example, cPAHs were found to be genotoxic, in agreement with available genotoxicity data.

Table II. Summary of the Cellular Proliferation of 14 Different PAHs in Binary Mixtures with BaP

Trial		Increase	No Change	Decline 1–2 Doses	Decline 3–4 Doses
BaP	Single			√	
Acy	Single			√	
	Binary	√	√		
	R.B	√	√		
Ac	Single		√		
	Binary		√		
	R.B	√	√		
BaA	Single			√	
	Binary	√	√		
	R.B	√	√		
BbF	Single				√
	Binary				√
	R.B	√	√		
BeP	Single		√		
	Binary		√		
	R.B			√	
BkF	Single		√		
	Binary		√		
	R.B		√		
Ch	Single		√		
	Binary			√	
	R.B	√	√		
Fla	Single			√	
	Binary	√	√		
	R.B	√	√		
Phe	Single		√		
	Binary	√	√		
	R.B	√	√		
Pyr	Single			√	
	Binary		√		
	R.B	√	√		
7,12-BaA	Single				√
	Binary		√		
	R.B				√
3,6-Phe	Single				√
	Binary			√	
	R.B		√		
9-Ac	Single			√	
	Binary		√		
	R.B			√	
9,10-Ac	Single				√
	Binary			√	
	R.B		√		

R.B = Reverse binary.

Table III. Summary of the Viability Results for 14 PAHs in Binary Mixtures with BaP

Trial		Increase	No Change	Decline 1–2 Doses	Decline 3–4 Doses
BaP	Single				√
Acy	Single			√	
	Binary				√
	R.B			√	
Ac	Single	√	√		
	Binary			√	
	R.B				√
BaA	Single				√
	Binary				√
	R.B				√
BbF	Single			√	
	Binary		√		
	R.B				√
BeP	Single			√	
	Binary				√
	R.B				√
BkF	Single				√
	Binary				√
	R.B			√	
Ch	Single				√
	Binary				√
	R.B				√
Fla	Single			√	
	Binary				√
	R.B			√	
Phe	Single		√		
	Binary				√
	R.B			√	
Pyr	Single			√	
	Binary		√		
	R.B			√	
7,12-BaA	Single				√
	Binary				√
	R.B				√
3,6-Phe	Single				√
	Binary				√
	R.B				√
9-Ac	Single			√	
	Binary				√
	R.B				√
9,10-Ac	Single	√		√	
	Binary	√			
	R.B				√

R.B = Reverse Binary.

3.3. Analyses of Mixture Interactions

Mixture analysis is most reliable with binary mixtures that vary in chemical concentrations, and where one of the components has a well-characterized response. The viability data were used to assess possible chemical interactions occurring between the PAHs in the binary mixtures using probit analysis. The viability data are normally distributed and have no anomalies among the doses, making for a homogenous mixture analysis. The genotoxicity was also used to analyze mixture interactions that may affect the frequency of MN. The frequencies of single PAHs were used to derive the expected additive response, and then compared to the observed response. Table V is a summary of the observed

Table IV. The Results of the MN Assay in Single PAH Concentrations and Various Combinations of Binary Mixtures

Chemical	Dose (BaP:PAH)	MN Freq/ 1,000 Cells	Cells Scored	Dying Cells (%)	Abnormal Nuclei (%)	Result (Positive/Negative)
Average control		0.01303	7,739	0.28	0.62	
Solvent control		0.01313	4,809	0.93	0.19	Negative
BaP only	1 ppm	0.02191	1,278	0.47	0.23	Positive
	10 ppm	0.01829	1,148	0.17	0.26	Positive
Acy	1 ppm	0.01873	995	1.18	0.89	Negative
	10 ppm	0.04020	776	1.77	0.38	Positive
	1:1	0.00462	1,733	0.84	1.80	Negative
	1:10	0.00695	1,870	0.68	1.26	Negative
	10:1	0.00851	1,997	0.15	0.10	Negative
Ac	1 ppm	0.04103	819	0.24	0.73	Positive
	10 ppm	0.05054	689	1.54	2.10	Positive
	1:1	0.01359	1,840	0.00	0.49	Positive
	1:10	0.00627	1,754	0.11	0.23	Negative
	10:1	0.01151	956	0.62	0.62	Negative
BaA	1 ppm	0.02386	936	0.42	2.08	Positive
	10 ppm	0.03704	880	0.66	1.88	Positive
	1:1	0.03166	1,611	0.74	0.55	Positive
	1:10	0.03972	1,435	1.23	0.82	Positive
	10:1	0.00644	1,707	0.18	0.23	Negative
BbF	1 ppm	0.07078	1,049	0.75	0.94	Positive
	10 ppm	0.20588	669	3.01	5.47	Positive
	1:1	0.03777	1,509	5.67	0.25	Positive
	1:10	0.08935	1,052	4.16	4.76	Positive
	10:1	0.01752	1,884	0.37	0.16	Positive
BeP	1 ppm	0.01691	946	1.94	1.63	Negative
	10 ppm	0.02389	921	1.60	0.21	Negative
	1:1	0.01050	1,904	0.05	0.31	Positive
	1:10	0.00813	1,107	0.00	0.00	Negative
	10:1	0.00787	1,907	0.11	0.11	Negative
BkF	1 ppm	0.01869	963	0.00	0.93	Negative
	10 ppm	0.02036	786	0.75	0.88	Negative
	1:1	0.00853	1,290	0.23	0.69	Negative
	1:10	0.01289	1,241	0.08	0.72	Negative
	10:1	0.01457	961	0.21	0.23	Negative
Ch	0.25 ppm	0.01278	2,034	0.20	0.39	Positive
	1 ppm	0.01126	2,043	0.05	0.15	Positive
	1: 0.25	0.01680	1,257	0.32	0.47	Negative
	1:1	0.00820	1,707	0.23	0.93	Negative
	10:1	0.00796	1,758	0.00	0.45	Negative
Fla	1 ppm	0.01419	916	0.22	0.11	Negative
	10 ppm	0.02605	499	0.00	0.40	Negative
	1:1	0.02407	1,370	0.93	0.65	Positive
	1:10	0.03813	813	0.60	1.21	Negative
	10:1	0.00438	914	0.11	0.61	Negative
Phe	1 ppm	0.02326	903	0.65	1.20	Negative
	10 ppm	0.02827	672	0.00	0.89	Negative
	1:1	0.02535	1,223	1.20	1.12	Positive
	1:10	0.01276	1,019	0.39	0.87	Negative
	10:1	0.01312	1,143	0.09	0.69	Negative
Pyr	1 ppm	0.01476	1,016	0.58	0.87	Negative
	10 ppm	0.01084	830	1.74	1.74	Negative
	1:1	0.01844	1,410	0.07	0.07	Positive
	1:10	0.01168	1,027	0.00	0.48	Negative
	10:1	0.01275	941	0.00	2.18	Negative
7,12-BaA	1 ppm	0.03333	870	1.24	0.79	Positive
	10 ppm	0.03521	852	0.35	0.32	Positive

(*Continued*)

Table IV. Continued

Chemical	Dose (BaP:PAH)	MN Freq/ 1,000 Cells	Cells Scored	Dying Cells (%)	Abnormal Nuclei (%)	Result (Positive/Negative)
	1:1	0.01799	1,056	0.99	24.01	Negative
	1:10	0.01629	921	0.37	31.96	Negative
	10:1	0.02483	886	1.45	0.00	Positive
3,6-Phe	1 ppm	0.02886	1,490	0.20	0.53	Positive
	10 ppm	0.02722	1,580	0.31	0.57	Positive
	1:1	0.00383	1,304	0.14	39.49	Positive
	1:10	0.00000	1,163	No result	49.30	None
	10:1	0.01736	1,037	0.48	0.67	Positive
9-Ac	1 ppm	0.01232	1,055	1.20	1.39	Negative
	10 ppm	0.01402	1,070	0.37	0.92	Negative
	1:1	0.02182	1,283	0.23	0.16	Positive
	1:10	0.03383	1,212	0.49	0.33	Positive
	10:1	0.01729	1,157	0.60	0.17	Positive
9,10-Ac	1 ppm	0.01704	1,643	0.24	0.78	Positive
	10 ppm	0.02270	881	0.99	1.98	Positive
	1:1	0.01794	2,341	0.04	0.64	Positive
	1:10	0.03133	1,532	0.26	0.65	Positive

Table V. Summary of Mixture Interactions for All PAH Analytes

Chemical	Viability	Genotoxicity
Acenaphthylene	A, S	A
Anthracene	A	A
Benz[a]anthracene	Ad, A	Ad, A
Benzo[b]fluoranthene	A, S	A
Benzo[e]pyrene	A	A
Benzo[k]fluoranthene	A, S	A
Chrysene	A, S	A
Fluoranthene	A	Ad, A
Phenanthrene	A, S	Ad, A
Pyrene	A	Ad, A
7,12-Dimethyl-benz[a]anthracene	A	A
3,6-Dimethyl-phenanthrene	Ad, A	A
9-Methylanthracene	Ad, S	Ad, A
9,10-Dimethyl-anthracene	A, S	A

Ad = addition; A = antagonism; S = synergism.

mixture interactions for both cell viability and genotoxicity to compare the effects seen in each assay. Mixture analyses revealed that complex interactions occur across chemical ratios and that mixture composition is a determining factor of interaction type. Additive toxicity was observed in very few trials, with nonadditive responses constituting the majority of interactions.

3.4. Quantitative Structure-Activity Relationships

QSAR can be a useful tool as a form of alternative toxicology. Because many PAHs lack toxicological data, the following models were developed to assess the potential efficacy of QSAR to predict toxic activity of the lesser well-known PAH congeners, such as the methylated PAHs. A maximum of four descriptors per model were assigned to avoid overfitting the data. Figs. 6–8 display the best models developed by the software's genetic function approximation (GFA) algorithm. The figures illustrate how closely the test data points are aligned to the developed model.

Tables VI and VII show how the equations can be modified to incorporate the component fractions from their EC_{50} values. These modified equations can utilize the descriptor values of each component in a mixture to predict the toxic activity for that specific mixture. These equations are different from the single PAH model because they are incorporating the nonadditive mixture interactions that were observed during toxicity experiments (Table V). The algorithms incorporate the single, binary, and reversed binary data, while also accounting for the observed mixture interactions that one would expect with specific chemical ratios.

Fig. 6 shows the algorithm and the regression of the best QSAR model to predict the EC_{50} of single PAHs. The model found the extended connectivity fingerprints (ECFPs), molecular weight, and the $\log K_{OW}$ to be significant factors for predicting the EC_{50} of these 15 PAHs. ECFPs are a very diverse set of topological descriptors that can describe an infinite array of molecular substructures and

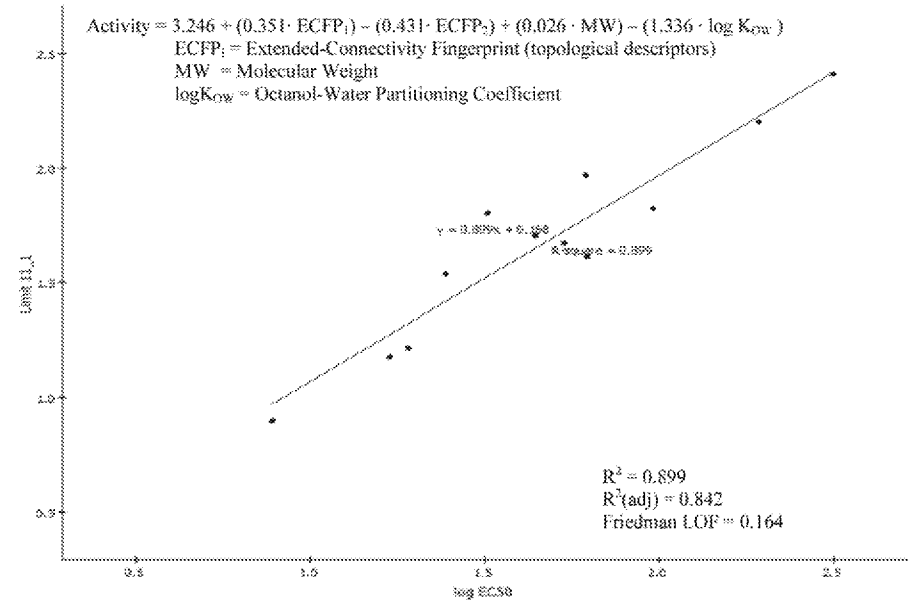

Fig. 6. A QSAR model predicts the EC_{50} of single PAH congeners. Along the *x*-axis are the experimental $logEC_{50}$ values, and along the *y*-axis are the predicted $logEC_{50}$ values. R^2 = correlation coefficients; Friedman LOF = lack of fit.

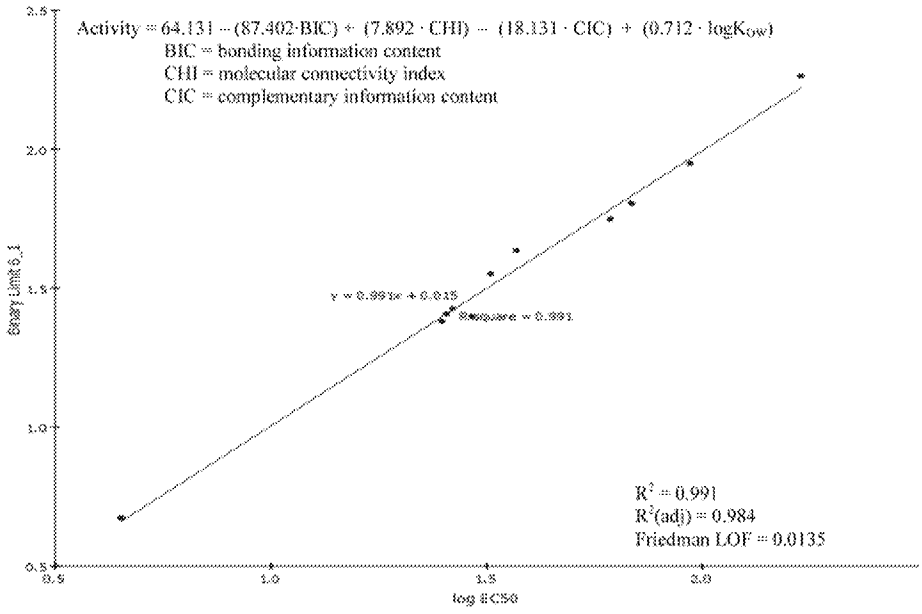

Fig. 7. The QSAR binary model displays the relationship of the experimental $logEC_{50}$ values (*x*-axis) to the predicted $logEC_{50}$ values generated by the model (*y*-axis).

connectivity between atoms of a chemical, such as the bay and fjord regions. The models' values are derived from the stereochemical arrangement of atoms within a chemical structure. Fig. 6 is the model for single dose-response data and is an acceptable predictive model of EC_{50} based on the large correlation coefficients and the LOF values of 0.164.

Figs. 7 and 8 display the models predicting the EC_{50} of binary mixtures where the components are known. Bonding information content (BIC) is an index describing the number of bonds and

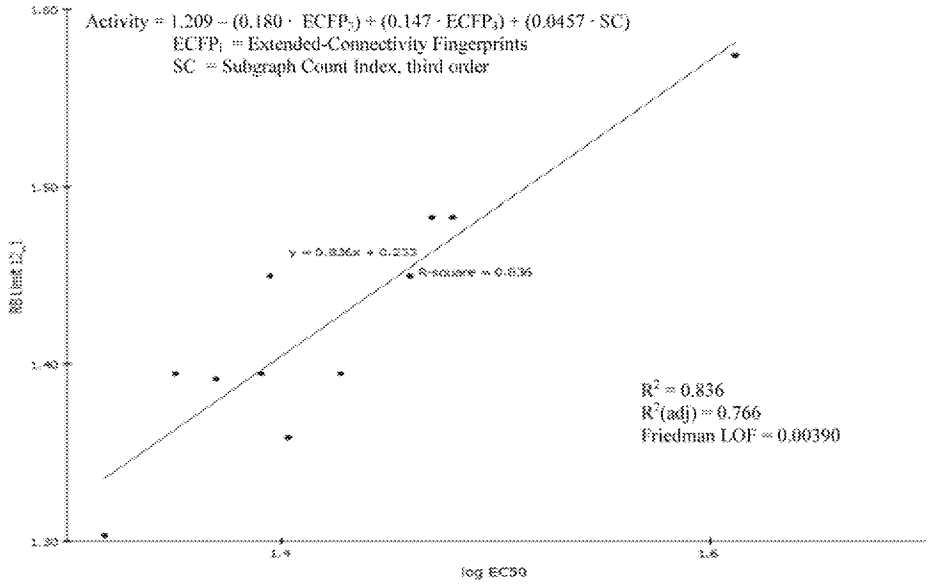

Fig. 8. The QSAR reverse binary model displays the relationship of the experimental $\log EC_{50}$ values (x-axis) to the predicted $\log EC_{50}$ values generated by the model (y-axis).

types of bonds in a chemical. The complementary information content (CIC) is a similar descriptor that relates molecular bonding to the atom makeup of a chemical. The Chi descriptor is another topological descriptor that interprets the angles of atom connectivity within the molecular graph of a chemical. Finally, the subgraph count (SC) is a descriptor relating to fractionated portion of a molecule, such as a string of hydrocarbon chains in a PAH. Topological descriptors are derived from the molecular graphs of specific chemicals, and weighted according to chemical composition, bond angles, and dimensional characteristics.[20] Topological descriptors, especially with planar PAHs, are shown to be significant molecular indices for predicting the biological index of a chemical class. These descriptors relate to the planar characteristics (2D) of PAHs, and the orientation about molecular bonds, highlighting that the planar nature of PAHs may affect the eventual toxicological fate of these PAHs in organisms. Finally, Figs. 7 and 8 are useful predictive models based on their correlation coefficients and their LOF values.

4. DISCUSSION

4.1. Mixtures

Chemicals in mixtures should act by the same mechanism if the toxicity is to conform to the additivity assumption.[27] Mixture interactions, however, are often caused by competition between toxicants at receptor sites.[27,29] As expected, the majority of our findings displayed nonadditive complex interactions occurring in mixtures. Table V shows that the majority of the mixtures exhibited an antagonistic relationship, and few mixtures showed additivity. When additivity was seen, it was coupled with another interaction in a mixture with different ratios.

Various studies using environmental mixtures that fall below their toxic thresholds were found to be synergistically toxic.[29] High doses are known to saturate the metabolic pathways where the chemicals may compete with each other for biotransformation, usually at the cytochrome P450 enzyme junction.[12] In this case, antagonism is the expected relationship between chemicals in the mixture because the enzymes cannot produce toxic intermediates quickly enough to demonstrate toxic additivity. One study conducted by Pohl *et al.* performed a weight-of-evidence analysis and concluded that the threshold for competitive inhibition of chemicals and mixtures may be the single most important factor for resulting toxicity.[29] In the case of PAHS, since there are numerous metabolic pathways that can lead to either toxicity or elimination, it is possible that antagonism will occur because the elimination pathways are favored at saturation over the toxic pathways.[12] Our

Table VI. Modified QSAR Models for Binary Mixtures to Account for the Component Ratios

Activity = 64.131 – Σ [(87.402•BIC) + (7.892 • CHI) – (18.131 • CIC) + (0.712 • $\log K_{OW}$)] $_{Components}$

Chemical	BaP Fraction	Modified Algorithms for Binary Mixtures:
Acenaphthylene	0.04	Activity = 64.131 + [–(87.4 * 0.04 * BIC) + (7.89 * 0.04 * CHI) – (18.1 * 0.04 * CIC) + (0.7 * 0.04 * $\log K_{OW}$)] $_{BaP}$ + [– (87.4 * 0.96 * BIC) + (7.89 * 0.96 * CHI) – (18.1 * 0.96 * CIC) + (0.7 * 0.96 * $\log K_{OW}$)] $_{Acy}$
Anthracene	0.02	Activity = 64.131 + [– (87.4 * 0.02 * BIC) + (7.89 * 0.02 * CHI) – (18.1 * 0.02 * CIC) +(0.7 * 0.02 * $\log K_{OW}$)]$_{BaP}$+ [– (87.4 * 0.98 * BIC) + (7.89 * 0.98 * CHI) – (18.1 * 0.98 * CIC) + (0.7 * 0.98 * $\log K_{OW}$)]$_{Ac}$
Benz[a]anthracene	0.03	Activity = 64.131 + [– (87.4 * 0.03 * BIC) + (7.89 * 0.03 * CHI) – (18.1 * 0.03 * CIC) + (0.7 * 0.03 * $\log K_{OW}$)]$_{BaP}$+ [– (87.4 * 0.97 * BIC) + (7.89 * 0.97 * CHI) – (18.1 * 0.97 * CIC) + (0.7 * 0.97 * $\log K_{OW}$)] $_{BaA}$
Benzo[b]fluoranthene	0.03	Activity = 64.131 + [– (87.4 * 0.030 * BIC) + (7.89 * 0.030 * CHI) – (18.1 * 0.030 * CIC) + (0.7 * 0.030*$\log K_{OW}$)]$_{BaP}$+ [– (87.4 * 0.97 * BIC) + (7.89 * 0.97 * CHI) – (18.1 * 0.97 * CIC) + (0.7 * 0.97 * $\log K_{OW}$)] $_{BbF}$
Benzo[e]pyrene	0.03	Activity = 64.131 + [– (87.4 * 0.03 * BIC) + (7.89 * 0.03 * CHI) – (18.1 * 0.03 * CIC) + (0.7 * 0.03 * $\log K_{OW}$)]$_{BaP}$+ [– (87.4 * 0.97 * BIC) + (7.89 * 0.97 * CHI) – (18.1 * 0.97 * CIC) + (0.7 * 0.97 * $\log K_{OW}$)] $_{BeP}$
Benzo[k]fluoranthene	0.04	Activity = 64.131 + [– (87.4 * 0.04 * BIC) + (7.89 * 0.04 * CHI) – (18.1 * 0.04 * CIC) + (0.7 * 0.04 * $\log K_{OW}$)]$_{BaP}$+ [– (87.4 * 0.96 * BIC) + (7.89 * 0.96 * CHI) – (18.1 * 0.96 * CIC) + (0.7 * 0.96 * $\log K_{OW}$)] $_{BkF}$
Chrysene	0.22	Activity = 64.131 + [– (87.4 * 0.22 * BIC) + (7.89 * 0.22 * CHI) – (18.1 * 0.22 * CIC) +(0.7 * 0.22 * $\log K_{OW}$)]$_{BaP}$+ [– (87.4 * 0.88 * BIC) + (7.89 * 0.88 * CHI) – (18.1 * 0.88 * CIC) + (0.7 * 0.88 * $\log K_{OW}$)] $_{Ch}$
Fluoranthene	0.04	Activity = 64.131 + [– (87.4 * 0.04 * BIC) + (7.89 * 0.04 * CHI) – (18.1 * 0.04 * CIC) + (0.7 * 0.04 * $\log K_{OW}$)]$_{BaP}$+ [– (87.4 * 0.96 * BIC) + (7.89 * 0.96 * CHI) – (18.1 * 0.96 * CIC) + (0.7 * 0.96 * $\log K_{OW}$)] $_{Fla}$
Phenanthrene	0.04	Activity = 64.131 + [– (87.4 * 0.04 * BIC) + (7.89 * 0.04 * CHI) – (18.1 * 0.04 * CIC) + (0.7 * 0.04 * $\log K_{OW}$)]$_{BaP}$+ [– (87.4 * 0.96 * BIC) + (7.89 * 0.96 * CHI) – (18.1 * 0.96 * CIC) + (0.7 * 0.96 * $\log K_{OW}$)] $_{Phe}$
Pyrene	0.01	Activity = 64.131 + [– (87.4 * 0.006 * BIC) + (7.89 * 0.006 * CHI) – (18.1 * 0.006 * CIC) + (0.7 * 0.006*$\log K_{OW}$)]$_{BaP}$+ [– (87.4 * 0.994 * BIC) + (7.89 * 0.994 * CHI) – (18.1 * 0.994 * CIC) + (0.7 * 0.994* $\log K_{OW}$)] $_{Pyr}$
7,12-Benz[a]anthracene	0.01	Activity = 64.131 + [– (87.4 * 0.01 * BIC) + (7.89 * 0.01 * CHI) – (18.1 * 0.01 * CIC) + (0.7 * 0.01 * $\log K_{OW}$)]$_{BaP}$+ [– (87.4 * 0.99 * BIC) + (7.89 * 0.99 * CHI) – (18.1 * 0.99 * CIC) + (0.7 * 0.99* $\log K_{OW}$)] $_{7,12\text{-}BaA}$
3,6-Phenanthrene	0.04	Activity = 64.131 + [– (87.4 * 0.04 * BIC) + (7.89 * 0.04 * CHI) – (18.1 * 0.04 * CIC) + (0.7 * 0.04 * $\log K_{OW}$)]$_{BaP}$+ [– (87.4 * 0.96 * BIC) + (7.89 * 0.96 * CHI) – (18.1 * 0.96 * CIC) + (0.7 * 0.96* $\log K_{OW}$)] $_{3,6\text{-}Phe}$
9-Anthracene	0.04	Activity = 64.131 + [– (87.4 * 0.04 * BIC) + (7.89 * 0.04 * CHI) – (18.1 * 0.04 * CIC) + (0.7 * 0.04 * $\log K_{OW}$)]$_{BaP}$+ [– (87.4 * 0.96 * BIC) + (7.89 * 0.96 * CHI) – (18.1 * 0.96 * CIC) + (0.7 * 0.96* $\log K_{OW}$)] $_{9\text{-}Ac}$
9,10-Anthracene	0.01	Activity = 64.131 + [– (87.4 * 0.01 * BIC) + (7.89 * 0.01 * CHI) – (18.1 * 0.01 * CIC) + (0.7 * 0.01 * $\log K_{OW}$)]$_{BaP}$+ [– (87.4 * 0.99 * BIC) + (7.89 * 0.99 * CHI) – (18.1 * 0.99 * CIC) + (0.7 * 0.99* $\log K_{OW}$)] $_{9,10\text{-}Ac}$

Table VII. Modified QSAR Models for Reversed Binary Mixtures to Account for the Component Ratios

	Activity = 1.209 – Σ [(0.180 • ECFP3) + (0.147 • ECFP4) + (0.0457 • SC)] $_{Components}$		
Chemical	BaP Fraction	PAH Fraction	Modified Algorithms for Reversed Binary Mixtures:
Acenaphthylene	0.96	0.04	Activity = 1.209 + [–(0.180 * 0.96 * ECFP3) + (0.147 * 0.96 * ECFP4) + (0.0457 * 0.96 * SC)] $_{BaP}$ + [–(0.180 * 0.04 * ECFP3) + (0.147 * 0.04 * ECFP4) + (0.0457 * 0.04 * SC)] $_{Acy}$
Anthracene	0.98	0.02	Activity = 1.209 + [–(0.180 * 0.98 * ECFP3) + (0.147 * 0.98 * ECFP4) + (0.0457 * 0.98 * SC)] $_{BaP}$ + [–(0.180 * 0.02 * ECFP3) + (0.147 * 0.02 * ECFP4) + (0.0457 * 0.02 * SC)] $_{Ac}$
Benz[a]anthracene	0.96	0.04	Activity = 1.209 + [–(0.180 * 0.96 * ECFP3) + (0.147 * 0.96 * ECFP4) + (0.0457 * 0.96 * SC)] $_{BaP}$ + (0.180 * 0.04 * ECFP3) + (0.147 * 0.04 * ECFP4) + (0.0457 * 0.04 * SC) $_{BaA}$
Benzo[b]fluoranthene	0.96	0.04	Activity = 1.209 + [–(0.180 * 0.96 * ECFP3) + (0.147 * 0.96 * ECFP4) + (0.0457 * 0.96 * SC)] $_{BaP}$ + [–(0.180 * 0.04 * ECFP3) + (0.147 * 0.04 * ECFP4) + (0.0457 * 0.04 * SC)] $_{BbF}$
Benzo[e]pyrene	0.96	0.04	Activity = 1.209 + [–(0.180 * 0.96 * ECFP3) + (0.147 * 0.96 * ECFP4) + (0.0457 * 0.96 * SC)] $_{BaP}$ + [–(0.180 * 0.04 * ECFP3) + (0.147 * 0.04 * ECFP4) + (0.0457 * 0.04 * SC)] $_{BeP}$
Benzo[k]fluoranthene	0.98	0.02	Activity = 1.209 + [–(0.180 * 0.98 * ECFP3) + (0.147 * 0.98 * ECFP4) + (0.0457 * 0.98 * SC)] $_{BaP}$ + [–(0.180 * 0.02 * ECFP3) + (0.147 * 0.02 * ECFP4) + (0.0457 * 0.02 * SC)] $_{BkF}$
Chrysene	0.95	0.05	Activity = 1.209 + [–(0.180 * 0.95 * ECFP3) + (0.147 * 0.95 * ECFP4) + (0.0457 * 0.95 * SC)] $_{BaP}$ + [–(0.180 * 0.05 * ECFP3) + (0.147 * 0.05 * ECFP4) + (0.0457 * 0.05 * SC)] $_{Ch}$
Fluoranthene	0.97	0.03	Activity = 1.209 + [–(0.180 * 0.97 * ECFP3) + (0.147 * 0.97 * ECFP4) + (0.0457 * 0.97 * SC)] $_{BaP}$ + [–(0.180 * 0.03 * ECFP3) + (0.147 * 0.03 * ECFP4) + (0.0457 * 0.03 * SC)] $_{Fla}$
Phenanthrene	0.96	0.04	Activity = 1.209 + [–(0.180 * 0.96 * ECFP3) + (0.147 * 0.96 * ECFP4) + (0.0457 * 0.96 * SC)] $_{BaP}$ + [–(0.180 * 0.04 * ECFP3) + (0.147 * 0.04 * ECFP4) + (0.0457 * 0.04 * SC)] $_{Phe}$
Pyrene	0.97	0.03	Activity = 1.209 + [–(0.180 * 0.97 * ECFP3) + (0.147 * 0.97 * ECFP4) + (0.0457 * 0.97 * SC)] $_{BaP}$ + [–(0.180 * 0.03 * ECFP3) + (0.147 * 0.03 * ECFP4) + (0.0457 * 0.03 * SC)] $_{Pyr}$
7,12-Benz[a]anthracene	0.96	0.04	Activity = 1.209 + [–(0.180 * 0.96 * ECFP3) + (0.147 * 0.96 * ECFP4) + (0.0457 * 0.96 * SC)] $_{BaP}$ + [–(0.180 * 0.04 * ECFP3) + (0.147 * 0.04 * ECFP4) + (0.0457 * 0.04 * SC)] $_{7,12\text{-}BaA}$
3,6-Phenanthrene	0.97	0.03	Activity = 1.209 + [–(0.180 * 0.97 * ECFP3) + (0.147 * 0.97 * ECFP4) + (0.0457 * 0.97 * SC)] $_{BaP}$ + [–(0.180 * 0.03 * ECFP3) + (0.147 * 0.03 * ECFP4) + (0.0457 * 0.03 * SC)] $_{3,6\text{-}Phe}$
9-Anthracene	0.95	0.05	Activity = 1.209 + [–(0.180 * 0.95 * ECFP3) + (0.147 * 0.95 * ECFP4) + (0.0457 * 0.95 * SC)] $_{BaP}$ + [–(0.180 * 0.05 * ECFP3) + (0.147 * 0.05 * ECFP4) + (0.0457 * 0.05 * SC)] $_{9\text{-}Ac}$
9,10-Anthracene	0.97	0.03	Activity = 1.209 + [–(0.180 * 0.97 * ECFP3) + (0.147 * 0.97 * ECFP4) + (0.0457 * 0.97 * SC)] $_{BaP}$ + [–(0.180 * 0.03 * ECFP3) + (0.147 * 0.03 * ECFP4) + (0.0457 * 0.03 * SC)] $_{9,10\text{-}Ac}$

mixture analyses observed mostly antagonism, indicating that such favoritism is evident. Further tests can be performed to confirm the specific mechanisms of actions, such as inducible enzymes and metabolite formation, but our current findings provide much information about possible interactions in PAH mixtures.

As mentioned, our experiments revealed an inhibitory trend where antagonism was observed in nearly all combinations of mixtures for both cell viability and genotoxicity. There have been very few published studies that examined cytotoxicity because most research is focused on cancer as the end point. However, cytotoxicity data are

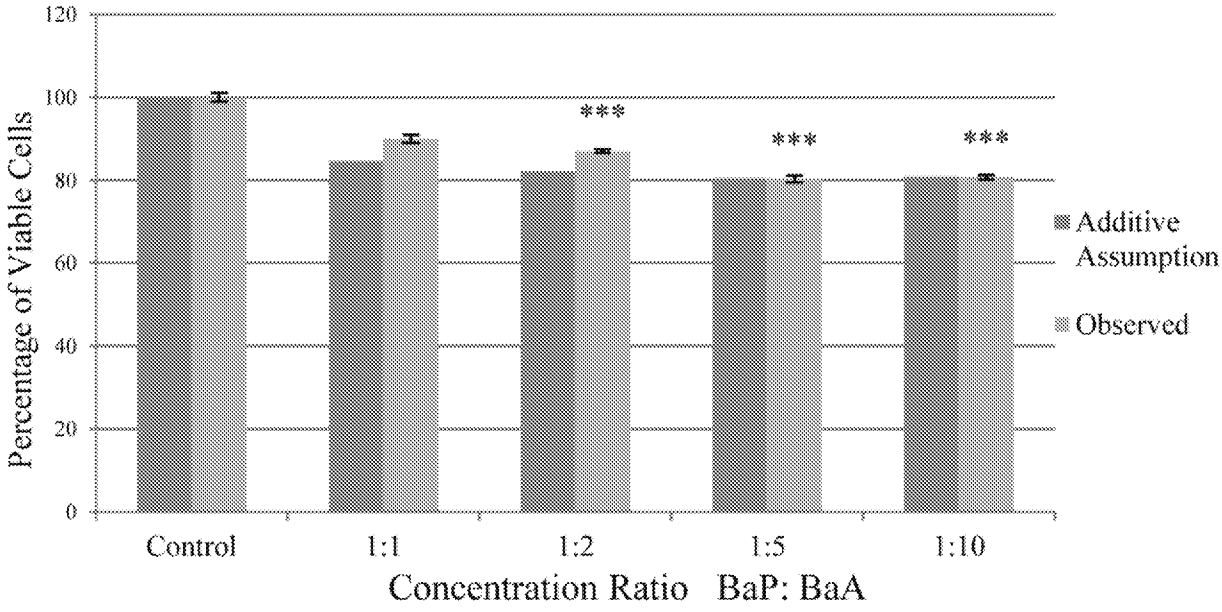

Fig. 9. A comparison of the expected additive response using the single chemical trial to the actual observed response in the binary mixture trial with benz[a]anthracene and BaP.

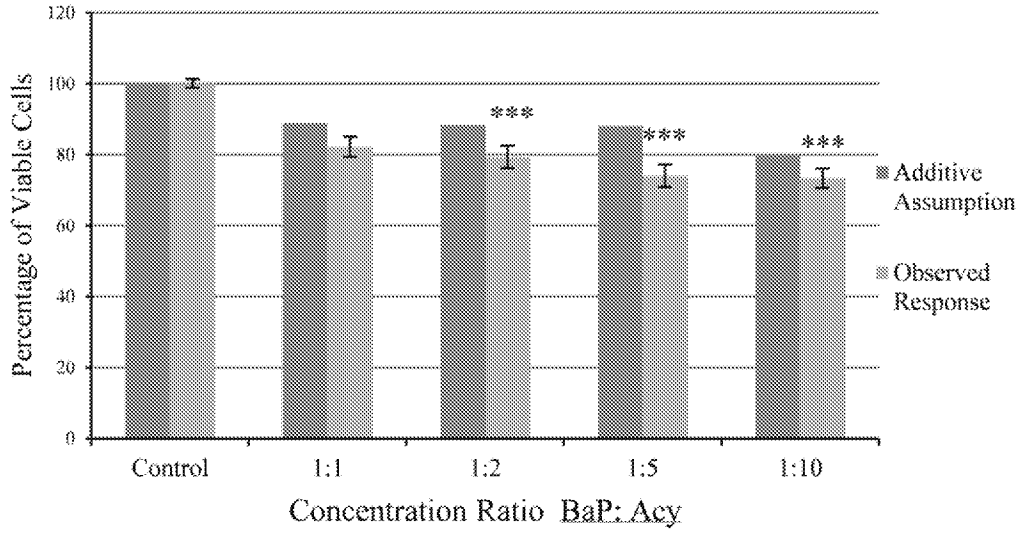

Fig. 10. Acenaphthylene displays a synergistic toxicity when compared to the expected additive response. In this mixture, BaP concentrations are held constant, and acenaphthylene varies.

useful because they indicate the first signs that a cell has endured an insult or injury (inhibition of cell growth/function, loss of membrane integrity, Lactose Dehydrogenase (LDH) leakage, etc.). The cytotoxicity data were normally distributed and provided excellent congruent data points between and within all doses. The mixture analysis revealed very few doses that had additive toxicity. One such example is the benz[a]anthracene viability trial (refer to Fig. 5C) when BaP concentrations were held constant in the mixture. Fig. 9 shows a comparison between the expected additive response to the observed response. The figure shows that they are closely aligned with each other.

Some PAHs displayed opposing mixture effects depending on the PAH in the mixture

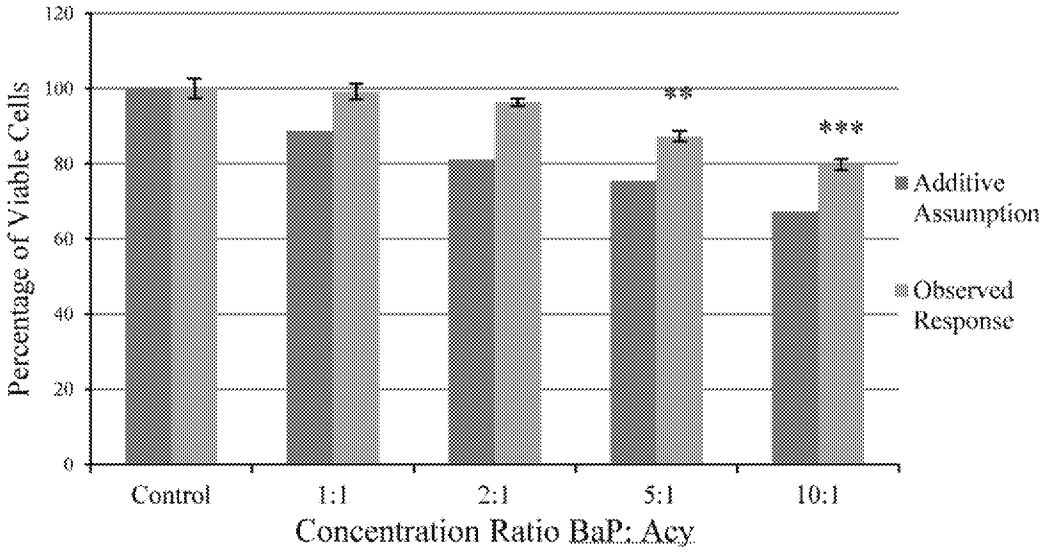

Fig. 11. The reverse binary mixture of acenaphthylene shows a clear antagonistic response when compared to both the expected additive response and the response of BaP alone. BaP concentrations vary and acenaphthylene is held constant.

that varied. Acenaphthylene, benzo[b]fluoranthene, benzo[k]fluoranthene, chrysene, phenanthrene, 9-methylanthracene, and 9,10-dimethylanthracene all showed both antagonism and synergism in binary mixtures. Acenaphthylene, for example, shows a clear synergistic response in mixtures where the concentration of acenaphthylene gradually increases and BaP is held at 1 mg/L. Figs. 10 and 11 display the two mixture trials where synergism and antagonism is observed in each.

The varying mixture effects may be the result of competition at receptor sites due to the ability of the component concentrations to outcompete each other. With the exception of 9,10-dimethylanthracene, all the binary trials showed synergism and the reversed binary showed antagonism. In binary trials, it follows that the PAH outcompetes BaP at receptor sites because the concentration is higher. The opposite is true for the reverse binary trials. This observation may be very important for elucidating the interactions between PAHs in complex mixtures. It could indicate that the varying affinities for the AhR binding site, which varies among PAHs, is a possible factor for predicting possible mixture interactions because it affects the rate of the appearance of toxic intermediates.[12] Other studies have observed nonadditive toxicities and have attributed interactions to competition at receptor sites.[11] Mahadevan *et al.*, for example, observed less than additive mixture toxicity by measuring the development of DNA adducts.[30] Tarantini *et al.* performed several genotoxicity tests and found that benzo[k]fluoranthene significantly inhibited the adduct formation with BaP.[13] Benzo[b]fluoranthene, however, increased the rate of DNA adduct formation.[13] Staal *et al.* found that the majority of the genotoxic response in mixtures with BaP, BbF, and fluoranthene were antagonistic, and the carcinogenic potency of PAHs in mixtures was significantly less than the predicted additive potency.[16] A different study observed antagonistic responses in human lung cancer cells (A549), in which the genotoxicity seen in complex mixtures was lower than single BaP and BkF trials.[31]

In agreement with these other studies, our genotoxicity results showed mainly antagonistic relationships between BaP and other PAHs. Additive responses were seen when the frequency of MN in the mixture was approximately equivalent to the sum frequencies of the individual components. However, toxic addition was always accompanied by another interaction depending on composition. Since BaP should always exert a statistically significant positive effect, any mixtures that yielded negative results (statistically insignificant from control) were automatically scored as antagonism. The majority of the mixture results showed that inhibition was a common effect, thereby inhibiting the genotoxicity of the mixture.

The MN test is time intensive and requires expensive fluorescence microscopy to score individual cells, which may limit sample size and scoring confidence. Despite limitations, this study scored an adequate sample size and furthermore the results were similar to other published literature. For example, cPAHs BaP, benz[a]anthracene, benzo[b]fluoranthene, and chrysene showed positive results in the MN test. In addition, anthracene, DMBA, and 9,10-dimethylanthracene were positive and in agreement with other published work that tested their genotoxicities.[24] Research on DMBA has seen much higher potencies than BaP.[32] This compound has a high rate of diol epoxide formation, but also has a decreased rate of induction of CYP1A1 when compared to BaP.[33] This means DMBA has a large potential for genotoxicity, but a concomitant possibility of reduced toxic action if the metabolizing enzymes are neither present nor inducible.

PAHs that have not yet been classified as carcinogenic were negative and include acenaphthylene, benzo[e]pyrene, fluoranthene, phenanthrene, and pyrene. Most of these PAHs have animal bioassay data that showed no tumor formation in test organisms (mice, rats, etc.), although there are a few exceptions.[34] Discrepancies in the MN results exist with benzo[k]fluoranthene. Benzo[k]fluoranthene has been classified as a probable human carcinogen given surmounting evidence in animal research.[34] However, the results of our MN test did not show a statistical increase in MN in single exposures to benzo[k]fluoranthene. This is likely because of random skewed sampling of the dosing groups, which can be symptomatic of small sample sizes. The sampled cells may not have been representative of the total cell population. It is likely that the weakly carcinogenic benzo[k]fluoranthene did not significantly induce the formation of MN, indicating that the assay may not have captured all genotoxic effects.

The chosen exposure period of 24 hours (with a single occurrence) could be an influential factor affecting genotoxicity. Since human exposures are chronic, many animal studies mimic chronic exposure scenarios but it is often less applicable *in vitro*. *In vitro* research often employs acute scenarios to examine DNA mutation, which is the first step of carcinogenesis. Tarantini *et al.* study performed an *in vitro* time-course study with BaP and binary mixtures with BbF and BkF and noted that the formation of DNA adducts peaked eight hours after exposure and plateaued.[13] Tarantini *et al.* also concluded that binary mixtures did not affect the overall frequency of adducts.[13] This may indicate that the chosen chemical exposure period may influence the rate of adduct formation, but not necessarily the frequency. Another study made an observation with a time-course study using an exposure period of 120 hours, stating that complex standard reference material coal tar mixture (#1597) caused a significant decline in BaP-DNA adducts when compared to cells exposed only to BaP.[30] Inhibition was most prominent during the first 48 hours of the exposure period.[30] Given that our studies utilized a 24-hour exposure period, it follows that many interactions were inhibitory.

Following BaP exposure, some cells significantly downregulate proteins that are involved in metastasis and tumor suppression.[35] For example, one study found that downregulated proteins were involved with apoptosis, cell structure, metabolism, and DNA synthesis.[36] Proteins involved with cell proliferation, growth, and differentiation were also upregulated.[36] Thus, cells are inhibited from apoptosis and vulnerable to abnormal growth, mutations, tumorigenesis, and metastasis that would otherwise be regulated normally.[37]

One limitation that was encountered in this study's genotoxicity testing was cell death. The concentrations that were used to score MN were meant to mimic hazardous contamination at National Priority List (NPL) sites. Scoring of benz[a]anthracene, benzo[b]fluoranthene, and 3,6-dimethylphenanthrene proved difficult because many cells were shrinking and dying. Cells exposed to 3,6-dimethylphenanthrene mixtures were often not scored because of cellular debris and cells lacked defined cellular and nuclear membranes.

An important factor to consider is the ability of the K-9 liver cells to express metabolizing enzymes. Kang *et al.* found that immortalized liver cells have higher concentrations of the CYP and Phase II enzymes necessary to metabolize and detoxify PAHs, which may contribute to higher proportions of detoxified PAHs when compared to other cell lines.[17] The study also found that the PAH mixtures were significantly cytotoxic to the cell lines tested, although the PAH mixtures used to dose the cells were extracted from dust samples containing other contaminants like heavy metals.[17] As discussed previously, the AhR, and CYP enzymes have been implicated as key predictors for the metabolization and interactions that occur in PAH mixtures. The additive assumption is not necessarily accurate for predicting mixture toxicity for human.[12,38] In

addition, mixture composition influences the type of interaction that may occur, which is evident by wide mixture variability and other studies' findings.[11,39]

A common pitfall for estimating PAH toxicity is the erratic variations of environmental mixtures and the many possible biotransformation pathways for PAHs in organisms. Toxicity could result from receptor competition, impaired cellular uptake, protein binding, impaired cellular functions, disrupted intercellular communications, mutations, among others.[14,16,40] Binary mixture data are a necessary first step in elucidating interactions in complex mixtures. More complex mixtures, such as ternary or quaternary, can further improve current knowledge on complex interactions. For example, Tarantini *et al.* saw complex genotoxic responses when comparing binary and ternary mixtures.[13] Mammalian studies have also seen a vast difference in toxicity and interactions.[27] Findings inform paradigms for evaluating mixtures and alternative toxicology methods to improve risk assessment of complex mixtures.

4.2. Quantitative Structure-Activity Relationships

Alternative toxicology is a useful tool for predicting toxicity of mixtures. QSAR modeling saves time, money, and experimental materials. Fig. 6 displays the model that predicts the EC_{50} of single PAHs based on the molecular structure of the analytes. The analyte list contained 15 congeners and produced a strong model with acceptable predictive power. With a correlation coefficient of about 90% and a LOF probability of 0.16, meaning the probability of accurately predicting the EC_{50} of PAHs. This promising model illustrates that QSAR could be a viable tool to bridge the data gaps for PAHs.

Recall that Figs. 7 and 8 show the QSAR models for the mixtures' EC_{50}. These mixture models also achieved strong correlations between the mixture EC_{50} and the molecular structures, particularly the binary mixture model (Fig. 7). Fig. 7 shows that the binary model closely fits the data, as evidenced by a R^2 value of 0.991 and R^2 (adj) of 0.984. These models are novel because they incorporate the mixture interactions evident in experimental data, something that has not yet been addressed. Some researchers have investigated the development of binary mixtures in QSAR modeling and have found that some simple alterations in the model equation may increase the predictive power.[14] For example, in the equations for the binary mixtures, a simple molar fraction or component ratio needs to be added into the polynomials to account for the mixture composition and then the equations are summed together (as seen in Tables VI and VII). Such modifications give the model flexibility by weighting the mixture components and allowing for customization. The descriptors for each component will then also apply to the summed model for the mixture. The algorithms are considerably strengthened when the mixture interactions and component ratios are accounted for. While our methods are designed to apply to simple binary PAH mixtures, they can be developed for more complex mixtures. This would save research time, materials, and funds while continuing to improve the accuracy of human health risk assessments regarding complex PAH exposures.

Another important factor in the QSAR models is the variation of descriptors for each model. The output revealed that the only intersection among the descriptors was $\log K_{OW}$ between the single and binary model. Every other descriptor was different among all three models, implying that the interactions cannot be estimated using one approach (i.e., additive assumption). This further illustrates the strength and usefulness of QSAR modeling to the prediction of risk associated with exposures to mixtures.

The wide variability of descriptors suggests that different molecular characteristics in mixture components may have shifting importance on the toxicity of the whole mixture, which suggests that QSAR mixture models that incorporate interactions are more robust. The toxicity of a single compound may be altered when a second or third competing compound is added to the exposure scenario. The varying mixture effects seen in the cytotoxicity and genotoxicity data correspond with this inference.

5. CONCLUSIONS

Many studies and agencies are currently revising the methods for assessing human health risks associated with PAH exposures. Due to the fact that humans are chronically exposed to PAH mixtures, it is important that PAHs be toxicologically characterized. The component-based methods include the assumptions that PAHs are biotransformed through similar metabolic pathways, and that toxicity is additive in mixtures. It has been observed, both by other researchers and in this study, however, that PAHs can exert their effects through a convoluted array of metabolic pathways, and that toxic addition is rare. The mixture-based methods possess their own set of limitations, including a wide variation of environmental mixture composition, as well as

various environmental factors affecting fate, partitioning, and degradation. It follows that there are many challenges for accurately assessing risks associated with PAH exposures.

The main objectives of this research were to elucidate the types of toxicological interactions occurring within simple PAH mixtures, and compare the observed effects to toxic addition. In summation, our *in vitro* studies saw minimal toxic additivity with nonadditive effects dominating most tested mixtures. The composition of these mixtures and which component varied influenced the type of interaction that occurred. This study confirmed that toxic addition is improbable in simple mixtures and more complex PAH mixtures are likely to see nonadditive responses when even more complex interactions occur between components.

The implications of our findings highlight the weaknesses of current approaches to estimating PAH toxicity. Current methodologies for human health risk assessments could be improved in various ways. First, environmental mixtures could be further studied to understand how the emission source affects mixture components, and how environmental matrices cause fluctuations in mixture compositions. The whole mixtures approach could be strengthened if toxicological data were available for a wider array of complex mixtures. Second, toxicological research could be performed on the vast number of PAH congeners that are not well known, as well as on simple mixtures to begin to understand interactions. Methylated PAHs, for example, have very little toxicological data available to incorporate into risk assessments. This study also saw success with the *in vitro* MN test, which could aid in focusing animal carcinogenesis studies on genotoxic chemicals. The consideration of *in vitro* research for prioritizing animal studies will cut down on research costs, material consumption, and animal lives. Such streamlining could improve the accuracy of risk estimation for the development of cancers in humans.

These suggestions can be time consuming and costly. This is undoubtedly why many data gaps remain for PAHs. Alternative toxicology can be most useful under these restrictions, saving time, funding, and expensive research materials. Developing QSAR models and improving QSAR software with newfound PAH mixture data will provide a cost-effective and timely supply of information regarding behavior of the entire class of PAHs. Such information adds to the little known facts about PAHs and their behavior in a biological system. It is possible PAH models can give valuable information about the mechanisms of biochemical action for PAHs. Furthermore, PAH QSAR models could expand the resources for monitoring techniques and screening, especially with the development of mixture models. QSAR may be a significant addition to traditional toxicological research, further focusing the experiments needed, and reducing the time and costs associated with this research, as well as bridging the data gaps for risk assessments.

6. FUTURE WORK

Future research will continue to characterize interactions of PAHs using ternary PAH mixtures of the same 15 chemical congeners used in this study. Furthermore, complex QSAR mixture analyses will be conducted that controls the selection of descriptors. The goal of future research is joint analyses that produce robust, interwoven QSAR models that incorporate the activity of PAH congeners and their observed behaviors in mixtures.

ACKNOWLEDGMENTS

This work was supported by C. Gus Glasscock, Jr., Endowed Fund for Excellence in Environmental Sciences in the College of Arts and Sciences at Baylor University, USA. The authors would like to thank Candace Tam for her assistance in this study.

REFERENCES

1. Fontana LF, Crapez MAC, de Figueiredo AG, Santos ES, Sobrinho da Silva F, Ribeiro AM, Martins da Rocha CC, Duarte A, Netto P. Characterization and distribution of polycyclic aromatic hydrocarbons in sediments from surui mangrove, Guanabara Bay, Rio de Janeiro, Brazil. Journal of Coastal Research, 2012; 28(1A):156–162.
2. Bruce ED, Abusalih AA, McDonald TJ, Autenrieth RL. Comparing deterministic and probabilistic risk assessments for sites contaminated by polycyclic aromatic hydrocarbons (PAHs). Journal of Environmental Science and Health, 2007; 42(6):697–706.
3. Stout SA, Graan TP. Quantitative source apportionment of PAHs in sediments of Little Menomonee River, Wisconsin: Weathered creosote versus urban background. Environmental Science & Technology, 2010; 44(8):2932–2939.
4. Yang TT, Lin ST, Lin TS, Hong WL. Characterization of polycyclic aromatic hydrocarbon emissions in the particulate phase from burning incenses with various atomic hydrogen/carbon ratios. Science of the Total Environment, 2012; 414:335–342.
5. Le Huu T, Nguyen Minh T, Takahashi S, Suzuki G, Viet PH, Subramanian A, Bulbule KA, Parthasarathy P, Ramanathan A, Tanabe S. Methylated and unsubstituted polycyclic aromatic hydrocarbons in street dust from Vietnam and India: Occurrence, distribution and in vitro toxicity evaluation. Environmental Pollution, 2014; 194:272–280.

6. Gehle K. Case Studies in Environmental Medicine: Toxicity of Polycyclic Aromatic Hydrocarbons (PAHs). Atlanta, GA: Agency for Toxic Substances and Disease Registry, 2009.
7. Schoeny R, Poirier K. Provisional Guidance for Quantitative Risk Assessment of Polycyclic Aromatic Hydrocarbons. Report No.: EPA/600/R-93/089. Washington, DC: U.S. Environmental Protection Agency, 1993.
8. Nisbet IC, Lagoy PK. Toxic equivalency factors (TEFs) for polycyclic aromatic hydrocarbons (PAHs). Regulatory Toxicology and Pharmacology, 1992; 16(3):290–300.
9. Reeves WR, Barhoumi R, Burghardt RC, Lemke SL, Mayura K, McDonald TJ, Phillips TD, Donnelly KC. Evaluation of methods for predicting the toxicity of polycyclic aromatic hydrocarbon mixtures. Environmental Science and Technology, 2001; 35(8):1630–1636.
10. Public Health Statement: Polycyclic Aromatic Hydrocarbons (PAHs). Atlanta, GA: Agency for Toxic Substances and Disease Registry, 1995.
11. Jarvis IW, Dreij K, Mattsson A, Jernstrom B, Stenius U. Interactions between polycyclic aromatic hydrocarbons in complex mixtures and implications for cancer risk assessment. Toxicology, 2014; 321:27–39.
12. Andrysik Z, Vondracek J, Marvanova S, Ciganek M, Neca J, Pencikova K, Mahadevan B, Topinka J, Baird WM, Kozubik A, Machala M. Activation of the aryl hydrocarbon receptor is the major toxic mode of action of an organic extract of a reference urban dust particulate matter mixture: The role of polycyclic aromatic hydrocarbons. Mutation Research, 2011; 714(1–2):53–62.
13. Tarantini A, Maitre A, Lefebvre E, Marques M, Rajhi A, Douki T. Polycyclic aromatic hydrocarbons in binary mixtures modulate the efficiency of benzo a pyrene to form DNA adducts in human cells. Toxicology, 2011; 279(1–3):36–44.
14. Altenburger R, Nendza M, Schuurmann G. Mixture toxicity and its modeling by quantitative structure-activity relationships. Environmental Toxicology and Chemistry, 2003; 22(8):1900–1915.
15. Andrada MF, Duchowicz PR, Castro EA. QSAR applications on polycyclic aromatic hydrocarbons and some derivatives. Current Organic Chemistry, 2013; 17(23):2872–2879.
16. Staal YC, Pushparajah DS, van Herwijnen MHM, Gottschalk RWH, Maas LM, Ioannides C, Van Van Schooten FJ, Van Delft JHM. Interactions between polycyclic aromatic hydrocarbons in binary mixtures: Effects on gene expression and DNA adduct formation in precision-cut rat liver slices. Mutagen, 2008; 23(6):491–499.
17. Kang YA, Cheung KC, Wong MH. Polycyclic aromatic hydrocarbons (PAHs) in different indoor dusts and their potential cytotoxicity based on two human cell lines. Environment International, 2010; 36(6):542–547.
18. Jarvis IWH, Bergvall C, Bottai M, Westerholm R, Stenius U, Dreij K. Persistent activation of DNA damage signaling in response to complex mixtures of PAHs in air particulate matter. Toxicology and Applied Pharmacology, 2013; 266(3): 408–418.
19. Mahadevan B, Luch A, Bravo CF, Atkin J, Steppan LB, Pereira C, Kerkvliet NI, Baird WM. Dibenzo a,l pyrene induced DNA adduct formation in lung tissue in vivo. Cancer Letters, 2005; 227(1):25–32.
20. Bruce ED, Autenrieth RL, Burghardt RC, Donnelly KC, McDonald TJ. Using quantitative structure-activity relationships (QSAR) to predict toxic endpoints for polycyclic aromatic hydrocarbons (PAH). Journal of Toxicology and Environmental Health-Part A, 2008; 71(16):1073–1084.
21. Cronin M, Walker J, Jaworska J, Comber MHI, Watts CD, Worth AP. Use of QSARs in international decision-making frameworks to predict ecological effects and environmental fate of chemical substances. Environmental Health Perspectives, 2003; 111(10):1376–1390.
22. Rieck P, Peters D, Hartmann C, Courtois Y. A new, rapid colorimetric assay for quantitative determination of cellular proliferation, growth inhibition, and viability. Journal of Tissue Culture Methods, 1993; 15:37–42.
23. Fenech M, Chang WP, Kirsch-Volders M, Holland N, Bonassi S, Zeiger E. Humn project: Detailed description of the scoring criteria for the cytokinesis-block micronucleus assay using isolated human lymphocyte cultures. Mutation Research-Genetic Toxicology and Environmental Mutagenesis, 2003; 534(1–2):65–75.
24. Matsushima T, Hayashi M, Matsuoka A, Ishidate M, Miura KF, Shimizu H, Suzuki Y, Morimoto K, Ogura H, Mure K, Koshi K, Sofuni T. Validation study of the in vitro micronucleus test in a Chinese hamster lung cell line (chl/iu). Mutagen, 1999; 14(6):569–580.
25. Kliesch U, Adler ID. Micronucleus test in bone-marrow of mice treated with 1-nitropropane, 2-nitropropane and cisplatin. Mutation Research, 1987; 192(3):181–184.
26. Finney DJ. The analysis of toxicity tests on mixtures of poisons. Annals of Applied Biology, 1942; 29(1):82–94.
27. Hertzberg R. Guidelines for the Health Risk Assessment of Chemical Mixtures. Report No.: EPA/630/R-98-002. Washington, DC: U.S. Environmental Protection Agency, 1986.
28. Song MK, Kim YJ, Song M, Choi HS, Park YK, Ryu JC. Formation of a 3,4-diol-1,2-epoxide metabolite of benz a anthracene with cytotoxicity and genotoxicity in a human in vitro hepatocyte culture system. Environmental Toxicology and Pharmacology, 2012; 33(2):212–225.
29. Pohl H, Mumtaz M, Scinicariello F, Hansen H. Binary weight-of-evidence evaluations of chemical interactions—15 years of experience. Regulatory Toxicology and Pharmacology, 2009; 54:264–271.
30. Mahadevan B, Marston CP, Luch A, Dashwood WM, Brooks E, Pereira C, Doehmer J, Baird WM. Competitive inhibition of carcinogen-activating cyp1a1 and CYP1b1 enzymes by a standardized complex mixture of PAH extracted from coal tar. International Journal of Cancer, 2007; 120(6):1161–1168.
31. Libalova H, Krckova S, Uhlirova K, Milcova A, Schmuczerova J, Ciganek M, Klema J, Machala M, Sram RJ, Topinka J. Genotoxicity but not the AHR-mediated activity of PAHs is inhibited by other components of complex mixtures of ambient air pollutants. Toxicology Letters, 2014; 225(3):350–357.
32. Galvan N, Teske DE, Zhou GD, Moorthy B, MacWilliams PS, Czuprynski CJ, Jefcoate CR. Induction of cyp1a1 and cyp1b1 in liver and lung by benzo(a)pyrene and 7,12-dimethylbenz(a)anthracene do not affect distribution of polycyclic hydrocarbons to target tissue: Role of AHR and cyp1b1 in bone marrow cytotoxicity. Toxicology and Applied Pharmacology, 2005; 202(3):244–257.
33. Gao J, Lauer FT, Dunaway S, Burchiel SW. Cytochrome p450 1b1 is required for 7,12-dimethylbenz(a)-anthracene (DMBA) induced spleen cell immunotoxicity. Toxicology Sciences, 2005; 86(1):68–74.
34. Mumtaz M, George J. Toxicological Profile for Polycyclic Aromatic Hydrocarbons. Atlanta, GA: Agency for Toxic Substances and Disease Registry, 1995.
35. Boess F, Kamber M, Romer S, Gasser R, Muller D, Albertini S, Suter L. Gene expression in two hepatic cell lines, cultured primary hepatocytes, and liver slices compared to the in vivo liver gene expression in rats: Possible implications for toxicogenomics use of in vitro systems. Toxicology Sciences, 2003; 73(2):386–402.
36. Oh S, Im H, Oh E, Lee J, Khim JY, Mun J, Kim Y, Lee E, Kim J, Sul D. Effects of benzo(a)pyrene on protein expression in jurkat t-cells. Proteomics, 2004; 4(11):3514–3526.
37. Asokkumar S, Naveenkumar C, Raghunandhakumar S, Kamaraj S, Anandakumar P, Jagam S, Devaki T. Antiproliferative and antioxidant potential of beta-ionone against

benzo(a)pyrene-induced lung carcinogenesis in Swiss albino mice. Molecular and Cellular Biochemistry, 2012; 363(1–2):335–345.
38. Marston CP, Pereira C, Ferguson J, Fischer K, Hedstrom O, Dashwood WM, Baird WM. Effect of a complex environmental mixture from coal tar containing polycyclic aromatic hydrocarbons (PAH) on the tumor initiation, PAH-DNA binding and metabolic activation of carcinogenic PAH in mouse epidermis. Carcinogenesis, 2001; 22(7):1077–1086.
39. Delgado-Saborit JM, Stark C, Harrison RM. Carcinogenic potential, levels and sources of polycyclic aromatic hydrocarbon mixtures in indoor and outdoor environments and their implications for air quality standards. Environment International, 2011; 37(2):383–392.
40. Tzekova A, Thuot R, Viau C. Correlation between biomarkers of polycyclic aromatic hydrocarbon exposure and electrophilic tissue burden in a rat model. Archives of Toxicology, 2004; 78(6):351–361.